PROMPT CURRICULUM LEARNING FOR EFFICIENT LLM POST-TRAINING

Anonymous authorsPaper under double-blind review

000

001

002003004

010 011

012

013

014

015

016

017

018

019

021

025

026027028

029

031

033

034

037

040

041

042

043

044

046

047

048

051

052

ABSTRACT

Reinforcement learning (RL) is widely used to post-train large language models for tasks such as mathematical reasoning and coding. However, the convergence of RL training remains sensitive to batching and prompt selection strategies. We investigate the factors that affect convergence, including batch size and prompt difficulty. Through large-scale experiments across multiple models and datasets, we show that there exists an optimal batch size that balances generation time and gradient quality, and that prompts of intermediate difficulty (where the model has roughly a 50% chance of success) are the most sample-efficient for model convergence. Motivated by these findings, we propose **Prompt Curriculum Learning** (PCL), a lightweight algorithm that selects intermediate-difficulty prompts using a learned value model. PCL avoids costly rollouts and efficiently guides training by focusing on the most informative samples. Empirically, PCL either achieves the highest performance or requires significantly less training time to reach comparable performance across a suite of benchmarks. Compared to using rollouts to filter, PCL is 12.1× and 16.9× faster on identifying intermediate-difficulty prompts when training on MATH and DeepScaleR respectively.

1 Introduction

Recent large language models (LLMs), such as OpenAI-o1 (OpenAI, 2024b) and DeepSeek-R1 (DeepSeek-AI, 2025), have demonstrated strong performance by producing long chain-of-thought (CoT) solutions (Wei et al., 2023; DeepSeek-AI, 2025; Zeng et al., 2025). A key driver of these improvements is reinforcement learning (RL) with rule-based rewards, using algorithms such as PPO (Schulman et al., 2017) and GRPO (Shao et al., 2024). By generating responses online from the current model, RL enables LLMs to self-explore and iteratively improve based on their own outputs.

Substantial effort has been devoted to improving both the performance and efficiency of RL training for LLMs (Brantley et al., 2025; Xu et al., 2025; An et al., 2025; Sun et al., 2025). A recurring insight across recent works (Yu et al., 2025; Zhang et al., 2025; Zheng et al., 2025) is that training on prompts of intermediate difficulty (i.e., neither too easy nor too hard for the current policy) yields significantly better data efficiency. However, existing approaches on identifying intermediate prompts typically rely on either rollouts from the current model or a dictionary that tracks average rewards from previous epochs. The former introduces substantial training overhead due to the high cost of online generation, while the latter suffers from off-policyness especially when the dataset is large. In addition, while these works primarily focus on prompt difficulty, many hyperparameters (e.g., batch size) can significantly affect convergence but remain underexplored in prior work.

In this paper, we conduct a systematic investigation into how prompt selection in conjunction with batch configuration impacts the convergence of RL training. We uncover two key findings. First, there exists an optimal batch size that achieves the best trade-off between faster generation time and smaller gradient noise. While larger batches reduce gradient noise and allow for higher learning rates, they also increase generation time, limiting update frequency. We identify a sweet spot at the transition point between sublinear and linear generation time growth, where convergence speed is maximized. Second, prompts of intermediate difficulty are the most effective for learning. When a prompt is too easy or too hard, gradient signals tend to vanish, leading to wasted compute. In contrast, prompts for which the model has a ~50% success rate yield the highest gradient norms

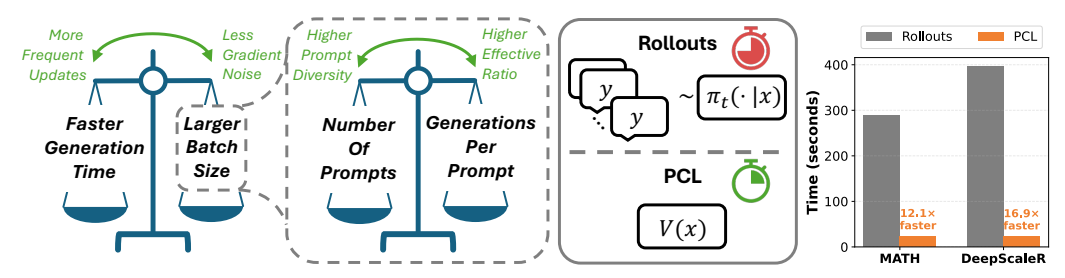


Figure 1: We conduct a systematic investigation of the trade-offs on generation time vs. batch size and number of prompts vs. generations per prompt. We identify an optimal batch size that achieves the best trade-off and discover that the prompts of intermediate difficulty are the most effective for learning. Building on these insights, we introduce **Prompt Curriculum Learning** (PCL), which trains a value model online for prompt filtering. Compared to the rollout-based filter method, PCL is $12.1\times$ and $16.9\times$ faster during prompt filtering when training on MATH and DeepScaleR respectively.

and require fewer samples to obtain informative updates. We validate this finding empirically across models, datasets, and batch configurations.

Building on these insights, we introduce **Prompt Curriculum Learning** (PCL), an efficient algorithm that dynamically selects prompts of intermediate difficulty using a value model. At each step, PCL samples a large pool of candidate prompts, predicts their expected reward with a single forward pass, and greedily selects those closest to a target threshold (e.g., 0.5). This approach avoids the overhead of rollout-based prompt filtering while also being much more on-policy than dictionary-based methods. We benchmark PCL across a wide range of models and datasets, including Qwen3-Base (1.7B, 4B, 8B) and Llama3.2-it (3B) on MATH, Olympiad-Bench, Minerva MATH, AMC, and AIME. Empirically, PCL either achieves the highest performance or requires substantially less training time to reach comparable performance.

2 Problem Setup

Let x denote a prompt (e.g., a math question), and let y denote a sampled solution of length |y| generated autoregressively from a policy π , i.e., $y \sim \pi(\cdot \mid x)$. We assume a binary reward function $r(x,y) \in \{0,1\}$, where r(x,y) = 1 if the final answer in y is correct and 0 otherwise. Since the reward is binary, we denote $p_{\pi}(x) \coloneqq \mathbb{E}_{y \sim \pi(\cdot \mid x)}[r(x,y)]$ as the probability of generating a correct answer from policy π on prompt x, and $A(x,y) \coloneqq r(x,y) - p_{\pi}(x)$ as the advantage. To optimize π , we adopt the purely on-policy variant of GRPO (Shao et al., 2024; DeepSeek-AI, 2025), without KL regularization to a fixed reference policy $\pi_{\rm ref}$ (Yu et al., 2025) and without standard deviation-based advantage regularization (Liu et al., 2025), by maximizing:

$$\mathbb{E}_{x \sim \mathcal{D}, y \sim \pi_t(\cdot \mid x)} \left[\frac{1}{|y|} \sum_{l=1}^{|y|} \frac{\pi(y_l \mid x, y_{< l})}{\pi_t(y_l \mid x, y_{< l})} A(x, y) \right], \tag{1}$$

where y_l denotes the l-th token in the generated sequence y. We adopt this formulation to eliminate the off-policyness during updates, clipping heuristics, and additional hyperparameters, which would complicate our analysis in the following section. We note that this is a **clean** RL objective that has the same gradient as policy gradient and can be directly derived from the original RL objective of maximizing expected reward: $\mathbb{E}_{x \sim \mathcal{D}, y \sim \pi(\cdot|x)}[r(x,y)]$. The derivation is provided in Appendix A.

3 Preliminary Investigations

In this section, we present a set of preliminary experiments that investigate the interplay between convergence, batch size, the number of prompts per batch, and the number of generations per prompt. We first define them in detail.

Batch size, denoted by b, refers to the total number of prompt–response pairs in a batch. In our purely on-policy setting, this number also corresponds to the total number of pairs used in a single update. The batch size is given by the product of the number of prompts and generations per prompt. Batch size directly affects the **generation time**, as larger batches require longer to generate.

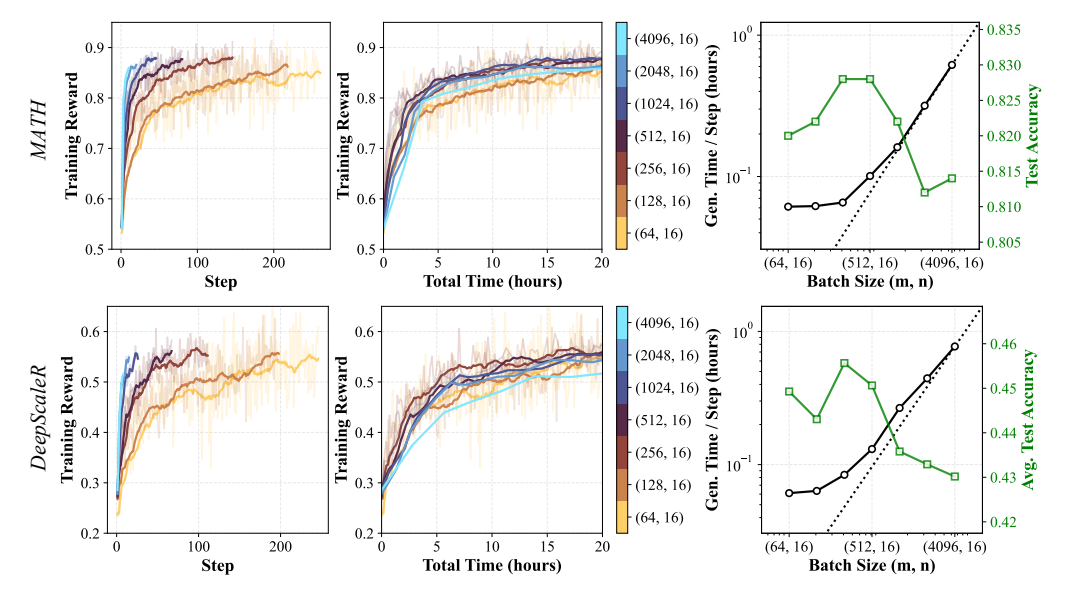


Figure 2: (Left / Middle) Training reward as a function of training steps and wall-clock time for Qwen3-4B-Base on MATH and DeepScaleR. The legend indicates the batch configuration in terms of (number of prompts m, generations per prompt n). (Right) Generation time per step and test accuracy across different batch sizes. The dashed line represents the linear increase that intercepts the origin and the generation time for the largest batch size. Both axes are in log scale. For key takeaways, refer to the paragraph headers in Section 3.1.

Number of prompts, denoted by m, refers to the number of unique prompts in a batch. This quantity is closely related to the **prompt diversity**. Increasing the number of prompts improves the diversity of the batch, which in turn reduces gradient noise and stabilizes learning.

Generations per prompt, denoted by n, refers to the number of responses generated for each prompt. These responses are used to estimate the expected reward, which is used to compute the advantage. The number of generations per prompt is related to the **effective ratio**, defined as the proportion of samples in the batch with non-zero advantages, i.e., the proportion of samples that contribute meaningful gradient signals. Increasing n improves the effective ratio. For example, for a particularly challenging prompt, if n=2, both responses may be incorrect, leading to zero advantage and zero gradient under the objective in Eq. 1. In contrast, for n=16 or 32, it is much more likely that at least one response is correct, resulting in a non-zero advantage and thus useful gradient updates. Therefore, increasing n would result in a more accurate advantage estimation and a higher effective ratio.

Convergence is defined as the final training or validation reward achieved under a fixed compute and time budget (e.g., number of GPUs and wall-clock time). A method exhibits faster convergence if, under the same computational resources, it reaches a higher reward. Convergence is influenced by generation time, prompt diversity, and effective ratio. Reducing generation time enables more frequent updates, while increasing prompt diversity and effective ratio reduces noise in the gradient and leads to more stable and efficient training.

Overall, these quantities exhibit a natural trade-off. On the one hand, reducing generation time enables more frequent updates within a fixed time budget, allowing the model to train on new rollouts from improved policies. On the other hand, increasing the number of prompts and generations per prompt reduces gradient noise with a higher signal-to-noise ratio. In the following experiments, we perform comprehensive ablations with around 100K A100 GPU hours to identify the optimal balance between these competing factors.

3.1 OPTIMAL BATCH SIZE

Experiment Setup. We conduct experiments on both MATH (Hendrycks et al., 2021) and Deep-ScaleR (Luo et al., 2025) datasets. For MATH, we evaluate on the standard MATH500 split. For Deep-ScaleR, we include evaluations on MATH500, Minerva Math (Lewkowycz et al., 2022), Olympiad-

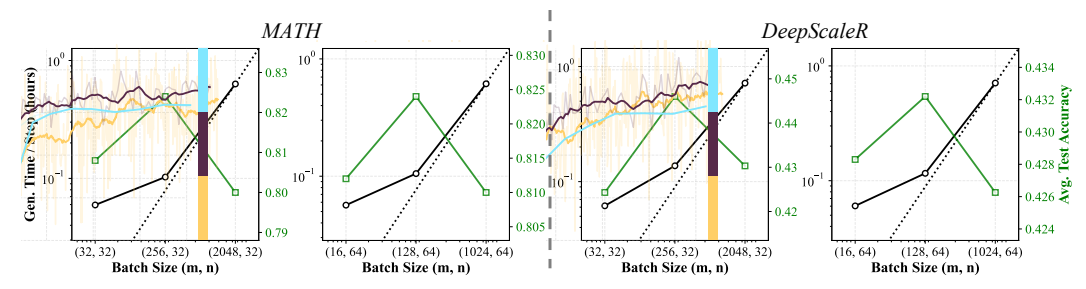


Figure 3: Generation time per step and test accuracy across different batch size combinations (number of prompts m, generations per prompt n) for Qwen3-4B-Base on MATH and DeepScaleR.

Bench (He et al., 2024), as well as competition-level benchmarks including AMC 23, AIME 24, and AIME 25. We report results across four models, Qwen3-1.7B-base, Qwen3-4B-base, Qwen3-8B-base, and Llama3.2-3B-it, covering two model families and a range of sizes. All models are trained with a context length of 4,096 tokens. We use a rule-based reward function based on math-verify (Hugging Face, 2024), which assigns a reward of +1 for correct ones and 0 for incorrect ones or generations that exceed the context limit. All experiments are implemented using the VERL (Sheng et al., 2025), a synchronous training setup that alternates between generation and optimization phases. For each batch size, we ablate to find the optimal learning rate with a total of 23 runs. Additional implementation and training details, including learning rate ablations, are provided in Appendix C.

The results for Qwen3-4B-Base are presented in Fig. 2 and 3, including training reward as a function of both training steps and wall-clock time (in hours), generation time per step using vLLM (Kwon et al., 2023), and test accuracy. For DeepScaleR runs, test accuracy is reported as the average across all six benchmarks. Full results are provided in Appendix D.

Larger batch sizes converge faster in terms of steps. As shown in Fig. 2 (Left), increasing the batch size consistently leads to faster convergence when measured in training steps. This is primarily because larger batches reduce gradient noise, allowing the use of higher learning rates without destabilizing training. The learning rates used in each configuration are listed in Tables 4 and 5.

Generation time grows sublinearly at first, then linearly. In Fig. 2 and 3, we plot generation time per step against batch size, alongside a dashed reference line representing linear growth (intersecting the origin). We observe that generation time initially increases sublinearly with batch size, and transitions to linear growth as batch size continues to increase. This behavior is expected: When the batch size is small, the generation time is dominated by the longest response in the batch. As batch size increases, compute utilization becomes the bottleneck, and generation time scales more linearly.

Optimal batch size occurs at the transition point from sublinear to linear scaling. From Fig. 2 (Middle / Right) and Fig. 3, there exists a sweet spot in batch size that yields the best convergence speed. Extremely small or large batch sizes lead to suboptimal performance. The optimal point for the fastest convergence tends to lie at the end of the sublinear regime and the beginning of the linear regime in generation time. Specifically, the optimal batch size in our setting is around 8K, achieved with combinations (m, n) = (512, 16), (256, 32), or (128, 64). In other words, the optimal batch size remains fixed, regardless of how it is factorized into m and n. We hypothesize that this sweet spot achieves a favorable balance: compared to smaller batch sizes, it can have linearly more generations with sublinear time growth; compared to larger batch sizes, it allows more frequent updates in the same amount of time. To ensure robustness, we validate this phenomenon across different model architectures and sizes, datasets, context lengths, hardware configurations, rollout engines (vLLM vs. SGLang), and batch configurations. Full results are provided in Appendix D. Having established an optimal batch size, the natural question is: How should we determine the optimal decomposition into the number of prompts and generations per prompt?

3.2 OPTIMAL NUMBER OF PROMPTS AND GENERATIONS PER PROMPT

We hypothesize that the optimal decomposition of the batch size is closely tied to the difficulty of the prompts. Specifically, for extremely easy or difficult prompts, a larger number of generations (n) may be necessary to achieve a high effective ratio. In contrast, for prompts of intermediate difficulty $(p(x) \approx 0.5)$, fewer generations may be sufficient.

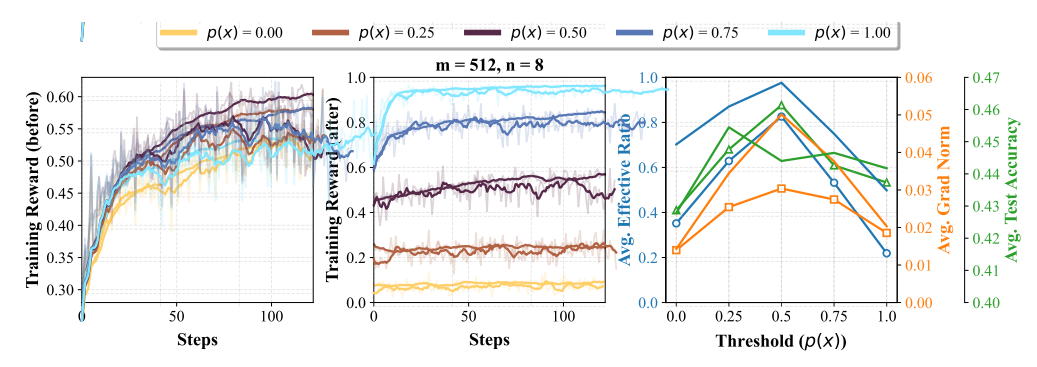


Figure 4: (Left) Training reward before downsampling in terms of step with number of prompts m=512 and generations per prompt n=8. (Middle) Training reward after downsampling. (Right) Average effective ratio and gradient norm over training steps, and average test accuracy of six benchmarks across different thresholds. For key takeaways, refer to Section 3.2.

Experiment Setup. We use DeepScaleR dataset and Qwen3-4B-Base, and train under different decompositions. To control prompt difficulty, for each batch we first sample 4m prompts and generate 4 responses for each prompt to estimate p(x), similar to Zhang et al. (2025). We then perform greedy downsampling to select m prompts that are closest to a specific difficulty threshold $p(x) \in \{0, 0.25, 0.5, 0.75, 1\}$, and sample n generations per selected prompt for training. We are not reusing the 4 responses to train to avoid selection-induced bias, which keeps the ablation on n comparable. We keep the total batch size fixed at $m \times n = 4096$ and ablate n from 2 to 128. All other experimental configurations remain the same. Full results are shown in Appendix D.

Downsampling successfully retains target-difficulty prompts. As shown in Fig. 4 (Left / Middle), our downsampling procedure effectively retains prompts around the specified threshold. This validates the experimental design and ensures that training focuses on prompts of controlled difficulty.

Higher n improves effective ratio and p(x) = 0.5 has the highest effective ratio. As shown in Fig. 4 (Right) and 5, increasing n consistently improves the effective ratio, and prompts with p(x) = 0.5 achieve high effective ratios even with relatively small n. For example, the effective ratio for n = 16 at p(x) = 0.5 is already higher than any other thresholds even with n = 128.

in Fig. 4 (Right) and 5, training on

n = 16 at p(x) = 0.5 is already higher than any other thresholds even with n = 128.

Figure 5: Average test accuracy. As shown

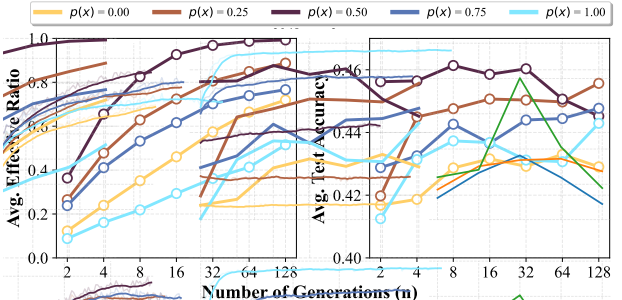


Figure 5: Average effective ratio over training steps and average test accuracy of six benchmarks under different thresholds p(x) and generations per prompt n.

prompts with p(x) = 0.5 yields the highest gradient norms and test accuracy. Interestingly, while increasing n benefits test accuracy for other difficulty levels, we find that for p(x) = 0.5, accuracy actually degrades beyond n = 32. We suspect this is due to reduced prompt diversity (i.e., smaller m), which increases gradient noise despite higher per-prompt sampling. Conversely, based on the previous section, since there exists an optimal batch size, focusing on p(x) = 0.5 allows us to use a smaller n and a higher m which improves prompt diversity and also maintains a high effective ratio. In other words, we could have the best of both worlds (effective ratio and prompt diversity) with p(x) = 0.5. Full results, including ablations across all configurations, are provided in Appendix D, and a theoretical connection of the gradient norm and p(x) is provided in Appendix E.

4 PCL: PROMPT CURRICULUM LEARNING

The previous section demonstrates that prompts of intermediate difficulty $(p(x) \approx 0.5)$ are the most sample-efficient for RL training. However, estimating the difficulty of each prompt using actual generations from the policy can be computationally expensive, as the generations for the filtered-out

Algorithm 1 PCL

Require: Number of prompts m, generations per prompt n, threshold τ , sampling parameter k

- 1: Initialize policy π_0 , value network $V^{\pi_{-1}}$
- 2: **for** t = 0 to T 1 **do**
- 3: Sample a batch with km prompts: $\mathcal{D}_{km} = \{x^i\}_{i=1}^{km} \subset \mathcal{D}$.
- 4: Select a batch of m prompts using value model: $\mathcal{D}_m = \underset{S \subseteq \mathcal{D}_{km}, |S|=m}{\arg \min} \sum_{x \in S} \left| V^{\pi_{t-1}}(x) \tau \right|.$
- 5: Generate for the batch: $\mathcal{D}_m = \left\{ (x^i, \{y^{i,j}\}_{j=1}^n) \right\}_{i=1}^m$ where $y^{i,j} \stackrel{\text{iid}}{\sim} \pi_t(\cdot \mid x^i)$
- 6: Update π_t to π_{t+1} using \mathcal{D}_m .
- 7: Update $V^{\pi_{t-1}}$ to V^{π_t} with loss in Eq. 2.
- 8: **end for**

prompts are wasted. To address this issue, we propose a lightweight and efficient alternative: Prompt Curriculum Learning (**PCL**), which leverages a learned value model during online RL to estimate prompt difficulty using a single forward pass, significantly reducing computational overhead.

At training iteration t, we begin by sampling a pool of km candidate prompts from the dataset where k is a hyperparameter. For each prompt x, we use a value model to predict its expected reward V(x), which approximates $p_{\pi}(x) = \mathbb{E}_{y \sim \pi(\cdot | x)}[r(x,y)]$. We then greedily select a subset of m prompts whose predicted values are closest to a target difficulty threshold τ (defaulting to 0.5), ensuring that the batch is focused on prompts of intermediate difficulty. For each selected prompt, we generate n responses using the current policy and perform standard policy gradient updates. To update the value model, we only use the generated responses and minimize the prediction error between the estimated value V(x) and the empirical average reward across the n generations:

$$\sum_{i=1}^{m} \left(V(x^i) - \frac{1}{n} \sum_{j=1}^{n} r(x^i, y^{i,j}) \right)^2.$$
 (2)

This allows us to improve the value model online, without requiring any additional rollouts. Since the value model only takes in the prompt as input which is typically less than 1K tokens in length for math, we find that both training and inference of the value model incur negligible cost and can be completed under 30 seconds for each step. The full algorithm is summarized in Algorithm 1. Note that the value model V in our algorithm is one step behind the policy π , which is acceptable since each update is small with $\pi_{t+1} \approx \pi_t$. We further discuss the alternatives in Section 6.

5 EXPERIMENTS

Models & Datasets. We use the same sets of models and datasets for experiments as Section 3. We use the same-sized model as the policy for the value model when running PCL. All runs use a 2-day time budget, except for Qwen3-8B-Base on DeepScaleR, which is trained for 3 days. We focus on m = 512 and n = 16 as it is one of the best combinations we found in terms of convergence. Unless otherwise noted, PCL uses $\tau = 0.5$ and k = 4. Similar to Wang et al. (2025b) and Zheng et al. (2025), we evaluate the model after training on every 4K prompts (8 steps), and report the performance of the checkpoint that obtains the best average performance.

Baselines. We compare PCL against five baselines. We include original GRPO, which performs no prompt filtering and uniformly samples prompts from the dataset. This serves as a standard baseline to assess the impact of filtering strategies. **Pre-filter** is a heuristic approach that leverages a fixed reference policy $\pi_{\rm ref}$ to estimate prompt difficulty and filters out easy or hard prompts. **Dynamic-sampling (DS)** (Yu et al., 2025) uses n rollouts per prompt to estimate p_{π} for km prompts and filters out prompts with $\hat{p}_{\pi} = 0$ or 1. **SPEED** (Zhang et al., 2025) improves upon DS by first using $n_{\rm init}$ rollouts to estimate where $n \ge n_{\rm init}$. It then performs filtering and generates the remaining $n - n_{\rm init}$ rollouts. **GRESO** (Zheng et al., 2025) keeps a dictionary of historical rewards based on generations from previous epochs and skips uninformative prompts using the dictionary. We tested GRESO on MATH but not on DeepScaleR, as DeepScaleR is large and limits the training to around 1 epoch under the compute budget which prevents the use of dictionary-based methods. DS, SPEED, and GRESO all keep sampling and generating until there is a full batch. Additional experiment details, including pseudo-codes and hyperparameters, are in Appendix F.

Table 1: **Results on MATH and DeepScaleR.** For each metric, the best-performing method is highlighted in **bold**, and the second-best is <u>underlined</u>. Time is the sum of training and generation time of the checkpoint that achieves the best average performance (excluding validation/checkpointing) in hours. For full DeepScaleR results across model sizes and families, refer to Appendix G.

MATH	Qwen3-8B-Base MATH500 Time		Qwen3-4B-Base MATH500 Time		Qwen3-1.7I MATH500	B-Base Time	Llama3.2-3B-it MATH500 Time	
π_{ref}	72.4	/	65.6	/	55.4	/	42.6	
GRPO	86.4	28.3	83.0	29.2	73.6	22.0	56.2	5.80
Pre-filter	84.8	17.1	81.6	27.1	73.4	13.5	55.4	7.47
DS	87.8	37.8	82.6	37.1	73.8	$\overline{27.6}$	56.8	19.3
SPEED	81.2	4.25	78.8	6.75	70.2	1.93	42.6	/
GRESO	87.2	29.1	83.0	33.1	73.4	17.6	56.6	7.37
PCL	88.2	37.2	83.4	<u>14.0</u>	73.8	24.8	57.8	14.3

	DeepScaleR	MATH500	Olymp.	Minerva Avg@4	AMC23 Avg@32	AIME24 Avg@32	AIME25 Avg@32	Avg.	Time
Base	π_{ref}	70.2	34.3	29.8	49.1	15.8	8.8	34.7	/
Ba	GRPO	87.2	57.9	45.3	70.1	25.3	22.7	51.4	43.0
8B-	Pre-filter	86.4	54.6	44.2	69.8	26.9	22.6	50.7	67.4
3-8	DS	87.2	55.3	45.7	71.5	24.9	24.2	51.5	69.5
wen3-	SPEED	82.4	46.4	40.3	66.6	21.1	15.7	45.5	19.3
ð	PCL	88.4	56.2	46.8	71.2	25.2	23.9	52.0	<u>41.8</u>

5.1 Convergence Comparison

PCL either achieves the highest performance or requires significantly less training time to reach comparable performance. The main results are summarized in Tables 1 (for full DeepScaleR results, refer to Appendix G). Compared to prior baselines, PCL consistently achieves the highest performance across all four models on the MATH dataset, and ranks either the first or second on DeepScaleR. DS requires significantly more time to converge, as it performs generation for all km prompts at each step with n generations per prompt. SPEED's efficient implementation pre-generates $n_{\rm init}$ rollouts at an earlier step with an old policy and uses them at the current step, treating them as if sampled from the current policy. While this approach reduces generation cost for estimating \hat{p}_{π} , it introduces severe off-policyness as the current policy is unlikely to generate those rollouts. We observe that most of the SPEED runs crashed within a few hours, leading to lower convergence time as it would crash afterward. On the other hand, GRESO also suffers from a high degree of off-policyness where the historical estimates are based on outdated policies from the last epoch and may not reflect the current model's performance, especially when the dataset is large.

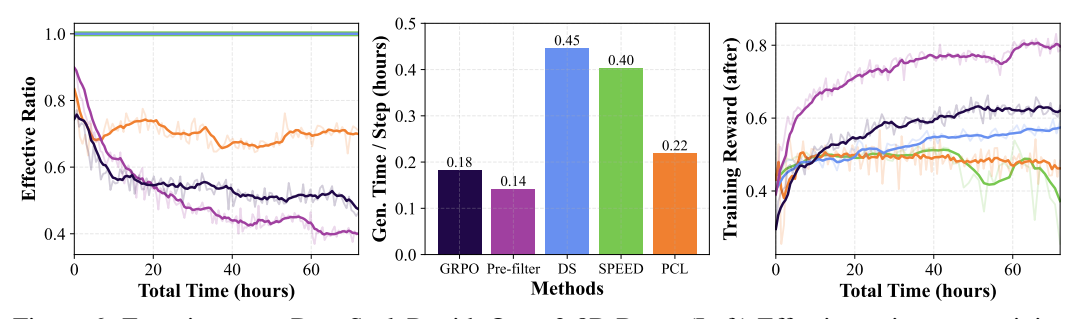
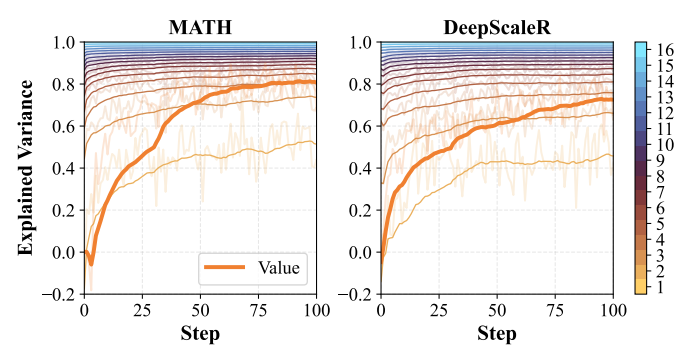


Figure 6: Experiment on DeepScaleR with Qwen3-8B-Base. (Left) Effective ratio w.r.t. training time across five methods. Refer to the middle plot for legend. (Middle) Average generation time per step throughout the training. (Right) Training reward after downsampling. PCL either has a higher effective ratio or a lower generation time, and is consistently training on p(x) = 0.5 prompts.

5.2 Analysis & Ablation

PCL consistently achieves either a higher effective ratio or a lower generation time, while maintaining a focus on p(x) = 0.5 prompts. To better understand the training dynamics of each method, we visualize the effective ratio, generation time per step, and training reward after filtering in



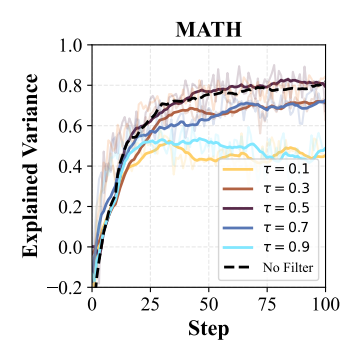


Figure 7: Explained variance of PCL's value model using 16 generations as the ground-truth difficulty (p(x)), and the explained variance using 1 to 16 generations to predict the difficulty $(\hat{p}(x))$ on MATH and DeepScaleR with two Qwen3-1.7B-Base models as policy and value model. The accuracy of the value model is similar to using around 3 generations to estimate.

Figure 8: Explained variance on MATH with Qwen3-1.7B-Base for PCL's value model with filtering on different thresholds (τ) and without filtering.

Fig. 6 when training Qwen3-8B-Base on DeepScaleR. PCL consistently maintains a higher effective ratio compared to GRPO and Pre-filter. While DS and SPEED achieve an effective ratio of 1 due to resampling, they require significantly higher generation time, with relative increase of 105% and 81.8% for DS and SPEED respectively. The slightly higher generation time of PCL compared to GRPO and Pre-filter is that harder prompts require longer generations, and, when the average accuracy of the model on the training set is higher than 0.5, PCL focuses on harder prompts than those two methods. Interestingly, the effective ratio for Pre-filter starts higher than GRPO but quickly drops below. This behavior comes from how Pre-filter selects prompts: it excludes very difficult ones based on $\pi_{\rm ref}$. As the policy improves during training, many previously difficult prompts transition into the intermediate-difficulty range (e.g., $p(x) \approx 0.5$) for the current model. However, because these prompts were previously filtered out, they are never revisited, causing Pre-filter to keep training on easy prompts from the perspective of the current policy. In addition, as shown in Fig. 6 (Right), PCL consistently focuses on intermediate-difficulty prompts throughout training (the training reward of PCL after filtering stays closely to 0.5), whereas other methods gradually shift toward easier prompts as the policy improves which is suboptimal based on the findings in Section 3.

The accuracy of the value model is similar to using 3 generations to estimate. To investigate the prediction accuracy of the value model, we compute the explained variance using the average reward of 16 generations as the ground-truth difficulty p(x). The explained variance is calculated as:

$$1 - \frac{\operatorname{Var}\left(\{p(x^{i}) - V(x^{i})\}_{i=1}^{m}\right)}{\operatorname{Var}\left(\{p(x^{i})\}_{i=1}^{m}\right)}$$
(3)

where Var denotes the variance. In addition, we also use the average reward of 1 to 16 generations as the predicted difficulty $\hat{p}(x)$ and compute their explained variance. The explained variances are computed on prompts randomly sampled from the dataset before filtering. The results on MATH and DeepScaleR with two Qwen3-1.7B-Base models as policy and value models are shown in Fig. 7. Since the prediction head of the value model is randomly initialized, the initial explained variance is very low. As training progresses, the value model improves steadily and achieves an explained variance comparable to using three rollouts per prompt for value estimation. Specifically, with km = 2048, generating n = 3 rollouts per prompt takes 288 seconds on MATH and 396 seconds on DeepScaleR per step. In contrast, training and inference with the value model require only 23.9 and 23.5 seconds respectively, achieving a $12.1\times$ speedup on MATH and a $16.9\times$ speedup on DeepScaleR. Results are visualized in Figure 1.

The accuracy of the value model with filtering at $\tau=0.5$ matches that of training without filtering. One might expect the value model to suffer from filtering, as the training data is biased toward prompts with estimated difficulty near the threshold τ , potentially limiting generalization. To investigate how the choice of threshold τ affects the accuracy of the value model, we ablate over $\tau \in \{0.1, 0.3, 0.5, 0.7, 0.9\}$. In addition, we train a baseline value model without any prompt filtering (i.e., GRPO but with a value model trained alongside the policy) using Qwen3-1.7B-Base for both the policy and value model on the MATH dataset. Results are presented in Fig. 8. We observe that the

value model achieves the highest prediction accuracy when $\tau=0.5$, with performance degrading as the threshold deviates further from 0.5 in either direction. Notably, the accuracy of the value model at $\tau=0.5$ is comparable to the no-filtering baseline, despite training on a filtered subset of prompts. We hypothesize that filtering at $\tau=0.5$ still captures a diverse set of reward outcomes, as it is the midpoint of the binary rewards. Moreover, if the average reward of the policy over the training data is not 0.5 (i.e., there is label imbalance), filtering around $\tau=0.5$ may implicitly rebalance the data, thus improving generalization. In contrast, filtering with extreme τ values (e.g., $\tau=0.1$ or $\tau=0.9$) selects only very easy or very hard prompts, leading to severe label imbalance and reduced predictive accuracy. A deeper theoretical understanding of why $\tau=0.5$ leads to such effective value model training is an interesting direction for future work.

PCL progressively focuses on harder prompts during training, despite a fixed threshold of $\tau = 0.5$. To better understand the training dynamics of PCL, we analyze how the difficulty of selected prompts evolves over time. Specifically, we use the initial reference policy π_{ref} to generate 16 responses for each prompt in DeepScaleR and compute the average reward, which serves as a proxy for prompt difficulty (i.e., lower average rewards indicate harder prompts). During training on Qwen3-8B-Base with PCL, we log the average π_{ref} -based reward for the filtered prompts at each training step. The results are shown in Fig. 9. For methods that do not perform prompt filtering (GRPO and Pre-filter), this average remains nearly constant, as these methods uniformly sample from the dataset. In contrast, for methods that apply filtering (DS, SPEED, and PCL), we observe a consistent downward trend in the π_{ref} -based reward of selected prompts. This indicates that these methods focus on increasingly harder prompts as training progresses. Although PCL maintains a fixed difficulty threshold of τ = 0.5, as the policy improves, previously hard prompts would now appear

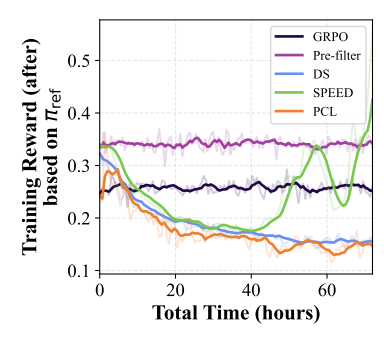


Figure 9: Training reward of PCL after filtering based on $\pi_{\rm ref}$ w.r.t. training time with DeepScaleR and Qwen3-8B-Base. PCL progressively focuses on harder prompts during training, despite a fixed threshold of $\tau = 0.5$.

intermediate (i.e., $\tau \approx 0.5$), allowing PCL to continually shift toward more challenging examples.

6 Discussions & Conclusion

PCL accelerates RL post-training by targeting two findings from our study: (1) there exists an optimal total batch size at the transition between sublinear and linear generation-time scaling, and (2) prompts of intermediate difficulty $(p(x) \approx 0.5)$ yield the highest gradient signal and sample efficiency. It trains a value model online to identify such prompts, avoiding the wasted rollouts of generation-based filtering (DS, SPEED) and the off-policyness of dictionary-based methods (GRESO). PCL either achieves the highest performance or requires significantly less training time to reach comparable performance. We include a discussion on related works and limitations in Appendix B and I.

While our experiments focus on binary correctness rewards, PCL naturally extends to non-binary scalar rewards. Since the value model V(x) estimates $\mathbb{E}_{y \sim \pi(\cdot|x)}[r(x,y)]$, non-binary r(x,y) only changes its range and the meaning of the target threshold τ . In addition, we note that PCL alternates updates between the policy and the value model, meaning that V^{π_t} is always one step behind the current policy π_{t+1} . In practice, this lag does not hinder performance, as the per-step policy updates are small with $\pi_t \approx \pi_{t+1}$. We also experimented with using importance sampling to correct for this lag by reweighting based on $\pi_{t+1}(y \mid x)/\pi_t(y \mid x)$, but it does not improve the accuracy of the value model and computing $\pi_{t+1}(y \mid x)$ is computationally expensive as y is thousands of tokens long.

We also highlight that prompt filtering methods rely on an implicit assumption of prompt-level generalization: training on a selected subset of prompts will improve performance on the filtered-out ones. For example, PCL assumes that training on intermediate-difficulty prompts leads to improvements on both easier and harder prompts, while DS and SPEED assume that gradually solving not-too-hard prompts enables the model to eventually handle harder ones. While this assumption holds in domains like math where problems often share structural similarities, it may not generalize to other domains. As such, filtering may bias the training distribution and hinder generalization to prompts outside the selected subset.

REFERENCES

- Arash Ahmadian, Chris Cremer, Matthias Gallé, Marzieh Fadaee, Julia Kreutzer, Olivier Pietquin, Ahmet Üstün, and Sara Hooker. Back to basics: Revisiting reinforce style optimization for learning from human feedback in llms, 2024. URL https://arxiv.org/abs/2402.14740.
- Chenxin An, Zhihui Xie, Xiaonan Li, Lei Li, Jun Zhang, Shansan Gong, Ming Zhong, Jingjing Xu, Xipeng Qiu, Mingxuan Wang, and Lingpeng Kong. Polaris: A post-training recipe for scaling reinforcement learning on advanced reasoning models, 2025. URL https://hkunlp.github.io/blog/2025/Polaris.
- Yoshua Bengio, Jérôme Louradour, Ronan Collobert, and Jason Weston. Curriculum learning. In *Proceedings of the 26th Annual International Conference on Machine Learning*, ICML '09, pp. 41–48, New York, NY, USA, 2009. Association for Computing Machinery. ISBN 9781605585161. doi: 10.1145/1553374.1553380. URL https://doi.org/10.1145/1553374.1553380.
- Kianté Brantley, Mingyu Chen, Zhaolin Gao, Jason D. Lee, Wen Sun, Wenhao Zhan, and Xuezhou Zhang. Accelerating rl for llm reasoning with optimal advantage regression, 2025. URL https://arxiv.org/abs/2505.20686.
- Zhipeng Chen, Yingqian Min, Beichen Zhang, Jie Chen, Jinhao Jiang, Daixuan Cheng, Wayne Xin Zhao, Zheng Liu, Xu Miao, Yang Lu, Lei Fang, Zhongyuan Wang, and Ji-Rong Wen. An empirical study on eliciting and improving r1-like reasoning models, 2025. URL https://arxiv.org/abs/2503.04548.
- Paul Christiano, Jan Leike, Tom B. Brown, Miljan Martic, Shane Legg, and Dario Amodei. Deep reinforcement learning from human preferences, 2023. URL https://arxiv.org/abs/1706.03741.
- Nirjhar Das, Souradip Chakraborty, Aldo Pacchiano, and Sayak Ray Chowdhury. Active preference optimization for sample efficient rlhf, 2025. URL https://arxiv.org/abs/2402.10500.
- DeepSeek-AI. Deepseek-r1: Incentivizing reasoning capability in llms via reinforcement learning, 2025. URL https://arxiv.org/abs/2501.12948.
- Hanze Dong, Wei Xiong, Deepanshu Goyal, Yihan Zhang, Winnie Chow, Rui Pan, Shizhe Diao, Jipeng Zhang, Kashun Shum, and Tong Zhang. Raft: Reward ranked finetuning for generative foundation model alignment, 2023. URL https://arxiv.org/abs/2304.06767.
- Wei Fu, Jiaxuan Gao, Xujie Shen, Chen Zhu, Zhiyu Mei, Chuyi He, Shusheng Xu, Guo Wei, Jun Mei, Jiashu Wang, Tongkai Yang, Binhang Yuan, and Yi Wu. Areal: A large-scale asynchronous reinforcement learning system for language reasoning, 2025. URL https://arxiv.org/abs/2505.24298.
- Zhaolin Gao, Jonathan Chang, Wenhao Zhan, Owen Oertell, Gokul Swamy, Kianté Brantley, Thorsten Joachims, Drew Bagnell, Jason D Lee, and Wen Sun. Rebel: Reinforcement learning via regressing relative rewards. *Advances in Neural Information Processing Systems*, 37:52354–52400, 2024.
- Zhaolin Gao, Wenhao Zhan, Jonathan D. Chang, Gokul Swamy, Kianté Brantley, Jason D. Lee, and Wen Sun. Regressing the relative future: Efficient policy optimization for multi-turn rlhf, 2025. URL https://arxiv.org/abs/2410.04612.
- Chaoqun He, Renjie Luo, Yuzhuo Bai, Shengding Hu, Zhen Leng Thai, Junhao Shen, Jinyi Hu, Xu Han, Yujie Huang, Yuxiang Zhang, Jie Liu, Lei Qi, Zhiyuan Liu, and Maosong Sun. Olympiadbench: A challenging benchmark for promoting agi with olympiad-level bilingual multimodal scientific problems, 2024. URL https://arxiv.org/abs/2402.14008.
- Dan Hendrycks, Collin Burns, Saurav Kadavath, Akul Arora, Steven Basart, Eric Tang, Dawn Song, and Jacob Steinhardt. Measuring mathematical problem solving with the math dataset, 2021. URL https://arxiv.org/abs/2103.03874.
- Jian Hu, Jason Klein Liu, Haotian Xu, and Wei Shen. Reinforce++: An efficient rlhf algorithm with robustness to both prompt and reward models, 2025. URL https://arxiv.org/abs/2501.03262.

```
Hugging Face. Math-verify. https://github.com/huggingface/Math-Verify, 2024.
```

- Kaixuan Ji, Guanlin Liu, Ning Dai, Qingping Yang, Renjie Zheng, Zheng Wu, Chen Dun, Quanquan Gu, and Lin Yan. Enhancing multi-step reasoning abilities of language models through direct q-function optimization. *arXiv preprint arXiv:2410.09302*, 2024.
- Amirhossein Kazemnejad, Milad Aghajohari, Eva Portelance, Alessandro Sordoni, Siva Reddy, Aaron Courville, and Nicolas Le Roux. VinePPO: Refining credit assignment in rl training of llms, 2025. URL https://arxiv.org/abs/2410.01679.
- Wouter Kool, Herke van Hoof, and Max Welling. Buy 4 reinforce samples, get a baseline for free! In *DeepRLStructPred@ICLR*, 2019. URL https://api.semanticscholar.org/CorpusID:198489118.
- Woosuk Kwon, Zhuohan Li, Siyuan Zhuang, Ying Sheng, Lianmin Zheng, Cody Hao Yu, Joseph E. Gonzalez, Hao Zhang, and Ion Stoica. Efficient memory management for large language model serving with pagedattention, 2023. URL https://arxiv.org/abs/2309.06180.
- Nathan Lambert, Jacob Morrison, Valentina Pyatkin, Shengyi Huang, Hamish Ivison, Faeze Brahman, Lester James V. Miranda, Alisa Liu, Nouha Dziri, Shane Lyu, Yuling Gu, Saumya Malik, Victoria Graf, Jena D. Hwang, Jiangjiang Yang, Ronan Le Bras, Oyvind Tafjord, Chris Wilhelm, Luca Soldaini, Noah A. Smith, Yizhong Wang, Pradeep Dasigi, and Hannaneh Hajishirzi. Tulu 3: Pushing frontiers in open language model post-training, 2025. URL https://arxiv.org/abs/2411.15124.
- Bruce W. Lee, Hyunsoo Cho, and Kang Min Yoo. Instruction tuning with human curriculum, 2024. URL https://arxiv.org/abs/2310.09518.
- Aitor Lewkowycz, Anders Andreassen, David Dohan, Ethan Dyer, Henryk Michalewski, Vinay Ramasesh, Ambrose Slone, Cem Anil, Imanol Schlag, Theo Gutman-Solo, Yuhuai Wu, Behnam Neyshabur, Guy Gur-Ari, and Vedant Misra. Solving quantitative reasoning problems with language models, 2022. URL https://arxiv.org/abs/2206.14858.
- Zhihang Lin, Mingbao Lin, Yuan Xie, and Rongrong Ji. CPPO: Accelerating the training of group relative policy optimization-based reasoning models, 2025. URL https://arxiv.org/abs/2503.22342.
- Zichen Liu, Changyu Chen, Wenjun Li, Penghui Qi, Tianyu Pang, Chao Du, Wee Sun Lee, and Min Lin. Understanding r1-zero-like training: A critical perspective, 2025. URL https://arxiv.org/abs/2503.20783.
- Michael Luo, Sijun Tan, Justin Wong, Xiaoxiang Shi, William Tang, Manan Roongta, Colin Cai, Jeffrey Luo, Tianjun Zhang, Erran Li, Raluca Ada Popa, and Ion Stoica. Deepscaler: Surpassing o1-preview with a 1.5b model by scaling rl, 2025. Notion Blog.
- Niklas Muennighoff, Zitong Yang, Weijia Shi, Xiang Lisa Li, Li Fei-Fei, Hannaneh Hajishirzi, Luke Zettlemoyer, Percy Liang, Emmanuel Candès, and Tatsunori Hashimoto. s1: Simple test-time scaling, 2025. URL https://arxiv.org/abs/2501.19393.
- William Muldrew, Peter Hayes, Mingtian Zhang, and David Barber. Active preference learning for large language models, 2024. URL https://arxiv.org/abs/2402.08114.
- OpenAI. GPT-4 technical report, 2024a. URL https://arxiv.org/abs/2303.08774.
- OpenAI. Learning to reason with llms. *OpenAI Blog Post*, 2024b.
 - Long Ouyang, Jeff Wu, Xu Jiang, Diogo Almeida, Carroll L. Wainwright, Pamela Mishkin, Chong Zhang, Sandhini Agarwal, Katarina Slama, Alex Ray, John Schulman, Jacob Hilton, Fraser Kelton, Luke Miller, Maddie Simens, Amanda Askell, Peter Welinder, Paul Christiano, Jan Leike, and Ryan Lowe. Training language models to follow instructions with human feedback, 2022. URL https://arxiv.org/abs/2203.02155.
 - Qwen. Qwen3 technical report, 2025. URL https://arxiv.org/abs/2505.09388.

- Rafael Rafailov, Archit Sharma, Eric Mitchell, Stefano Ermon, Christopher D. Manning, and Chelsea Finn. Direct preference optimization: Your language model is secretly a reward model, 2024. URL https://arxiv.org/abs/2305.18290.
- Lorenz Richter, Ayman Boustati, Nikolas Nüsken, Francisco Ruiz, and Omer Deniz Akyildiz. Vargrad: a low-variance gradient estimator for variational inference. *Advances in Neural Information Processing Systems*, 33:13481–13492, 2020.
- John Schulman, Filip Wolski, Prafulla Dhariwal, Alec Radford, and Oleg Klimov. Proximal policy optimization algorithms. *arXiv* preprint arXiv:1707.06347, 2017.
- Zhihong Shao, Peiyi Wang, Qihao Zhu, Runxin Xu, Junxiao Song, Xiao Bi, Haowei Zhang, Mingchuan Zhang, YK Li, Y Wu, et al. Deepseekmath: Pushing the limits of mathematical reasoning in open language models. *arXiv preprint arXiv:2402.03300*, 2024.
- Guangming Sheng, Chi Zhang, Zilingfeng Ye, Xibin Wu, Wang Zhang, Ru Zhang, Yanghua Peng, Haibin Lin, and Chuan Wu. Hybridflow: A flexible and efficient rlhf framework. In *Proceedings of the Twentieth European Conference on Computer Systems*, EuroSys '25, pp. 1279–1297. ACM, March 2025. doi: 10.1145/3689031.3696075. URL http://dx.doi.org/10.1145/3689031.3696075.
- Taiwei Shi, Yiyang Wu, Linxin Song, Tianyi Zhou, and Jieyu Zhao. Efficient reinforcement finetuning via adaptive curriculum learning, 2025. URL https://arxiv.org/abs/2504.05520.
- Yifan Sun, Jingyan Shen, Yibin Wang, Tianyu Chen, Zhendong Wang, Mingyuan Zhou, and Huan Zhang. Improving data efficiency for llm reinforcement fine-tuning through difficulty-targeted online data selection and rollout replay, 2025. URL https://arxiv.org/abs/2506.05316.
- Kimi Team. Kimi k1.5: Scaling reinforcement learning with llms, 2025a. URL https://arxiv.org/abs/2501.12599.
- Kimi Team. Kimi k2: Open agentic intelligence, 2025b. URL https://arxiv.org/abs/2507.20534.
- Huaijie Wang, Shibo Hao, Hanze Dong, Shenao Zhang, Yilin Bao, Ziran Yang, and Yi Wu. Offline reinforcement learning for llm multi-step reasoning. *arXiv preprint arXiv:2412.16145*, 2024.
- Liangyu Wang, Huanyi Xie, Xinhai Wang, Tianjin Huang, Mengdi Li, and Di Wang. Infinite sampling: Efficient and stable grouped rl training for large language models, 2025a. URL https://arxiv.org/abs/2506.22950.
- Yiping Wang, Qing Yang, Zhiyuan Zeng, Liliang Ren, Liyuan Liu, Baolin Peng, Hao Cheng, Xuehai He, Kuan Wang, Jianfeng Gao, Weizhu Chen, Shuohang Wang, Simon Shaolei Du, and Yelong Shen. Reinforcement learning for reasoning in large language models with one training example, 2025b. URL https://arxiv.org/abs/2504.20571.
- Jason Wei, Xuezhi Wang, Dale Schuurmans, Maarten Bosma, Brian Ichter, Fei Xia, Ed Chi, Quoc Le, and Denny Zhou. Chain-of-thought prompting elicits reasoning in large language models, 2023. URL https://arxiv.org/abs/2201.11903.
- Liang Wen, Yunke Cai, Fenrui Xiao, Xin He, Qi An, Zhenyu Duan, Yimin Du, Junchen Liu, Lifu Tang, Xiaowei Lv, Haosheng Zou, Yongchao Deng, Shousheng Jia, and Xiangzheng Zhang. Light-r1: Curriculum sft, dpo and rl for long cot from scratch and beyond, 2025. URL https://arxiv.org/abs/2503.10460.
- Ronald J. Williams. Simple statistical gradient-following algorithms for connectionist reinforcement learning. *Mach. Learn.*, 8(3–4):229–256, may 1992. ISSN 0885-6125. doi: 10.1007/BF00992696. URL https://doi.org/10.1007/BF00992696.
- Bo Wu, Sid Wang, Yunhao Tang, Jia Ding, Eryk Helenowski, Liang Tan, Tengyu Xu, Tushar Gowda, Zhengxing Chen, Chen Zhu, Xiaocheng Tang, Yundi Qian, Beibei Zhu, and Rui Hou. Llamarl: A distributed asynchronous reinforcement learning framework for efficient large-scale llm training, 2025. URL https://arxiv.org/abs/2505.24034.

- Mengzhou Xia, Sadhika Malladi, Suchin Gururangan, Sanjeev Arora, and Danqi Chen. Less: Selecting influential data for targeted instruction tuning, 2024. URL https://arxiv.org/abs/2402.04333.
- Wei Xiong, Jiarui Yao, Yuhui Xu, Bo Pang, Lei Wang, Doyen Sahoo, Junnan Li, Nan Jiang, Tong Zhang, Caiming Xiong, and Hanze Dong. A minimalist approach to llm reasoning: from rejection sampling to reinforce, 2025. URL https://arxiv.org/abs/2504.11343.
- Yixuan Even Xu, Yash Savani, Fei Fang, and Zico Kolter. Not all rollouts are useful: Downsampling rollouts in llm reinforcement learning, 2025. URL https://arxiv.org/abs/2504.13818.
- An Yang, Beichen Zhang, Binyuan Hui, Bofei Gao, Bowen Yu, Chengpeng Li, Dayiheng Liu, Jianhong Tu, Jingren Zhou, Junyang Lin, Keming Lu, Mingfeng Xue, Runji Lin, Tianyu Liu, Xingzhang Ren, and Zhenru Zhang. Qwen2.5-math technical report: Toward mathematical expert model via self-improvement, 2024. URL https://arxiv.org/abs/2409.12122.
- Yixin Ye, Zhen Huang, Yang Xiao, Ethan Chern, Shijie Xia, and Pengfei Liu. Limo: Less is more for reasoning, 2025. URL https://arxiv.org/abs/2502.03387.
- Qiying Yu, Zheng Zhang, Ruofei Zhu, Yufeng Yuan, Xiaochen Zuo, Yu Yue, Weinan Dai, Tiantian Fan, Gaohong Liu, Lingjun Liu, Xin Liu, Haibin Lin, Zhiqi Lin, Bole Ma, Guangming Sheng, Yuxuan Tong, Chi Zhang, Mofan Zhang, Wang Zhang, Hang Zhu, Jinhua Zhu, Jiaze Chen, Jiangjie Chen, Chengyi Wang, Hongli Yu, Yuxuan Song, Xiangpeng Wei, Hao Zhou, Jingjing Liu, Wei-Ying Ma, Ya-Qin Zhang, Lin Yan, Mu Qiao, Yonghui Wu, and Mingxuan Wang. Dapo: An open-source llm reinforcement learning system at scale, 2025. URL https://arxiv.org/abs/2503.14476.
- Yu Yue, Yufeng Yuan, Qiying Yu, Xiaochen Zuo, Ruofei Zhu, Wenyuan Xu, Jiaze Chen, Chengyi Wang, TianTian Fan, Zhengyin Du, Xiangpeng Wei, Xiangyu Yu, Gaohong Liu, Juncai Liu, Lingjun Liu, Haibin Lin, Zhiqi Lin, Bole Ma, Chi Zhang, Mofan Zhang, Wang Zhang, Hang Zhu, Ru Zhang, Xin Liu, Mingxuan Wang, Yonghui Wu, and Lin Yan. Vapo: Efficient and reliable reinforcement learning for advanced reasoning tasks, 2025. URL https://arxiv.org/abs/2504.05118.
- Weihao Zeng, Yuzhen Huang, Qian Liu, Wei Liu, Keqing He, Zejun Ma, and Junxian He. Simplerlzoo: Investigating and taming zero reinforcement learning for open base models in the wild, 2025. URL https://arxiv.org/abs/2503.18892.
- Ruiqi Zhang, Daman Arora, Song Mei, and Andrea Zanette. Speed-rl: Faster training of reasoning models via online curriculum learning, 2025. URL https://arxiv.org/abs/2506.09016.
- Haizhong Zheng, Yang Zhou, Brian R. Bartoldson, Bhavya Kailkhura, Fan Lai, Jiawei Zhao, and Beidi Chen. Act only when it pays: Efficient reinforcement learning for llm reasoning via selective rollouts, 2025. URL https://arxiv.org/abs/2506.02177.
- Banghua Zhu, Michael Jordan, and Jiantao Jiao. Principled reinforcement learning with human feedback from pairwise or k-wise comparisons. In *International Conference on Machine Learning*, pp. 43037–43067. PMLR, 2023.

Appendix

CONTENTS

A	Prol	olem Se	tup Details	15
В	Rela	ited Wo	rk	16
C	Prel	iminary	Investigation Details	17
	C .1	Datase	t Details	17
	C.2	Model	Details	17
	C.3	Rewar	d Details	17
	C.4	Evalua	tion Details	17
	C.5	Compl	ete List of Experiments	18
D	Prel	iminary	Investigation Complete Results	21
	D.1	Compl	ete Results for Section 3.1	21
		D.1.1	Results with varying m	21
		D.1.2	Results with varying m and n	23
		D.1.3	Results with a different context length	25
		D.1.4	Results with a different hardware configuration	26
		D.1.5	Results with a different inference engine	27
	D.2	Compl	ete Results for Section 3.2	28
E	Con	nection	between $p(x)$ and Gradient Magnitude	31
F	Exp	eriment	t Details	32
	F.1	Baselin	nes Algorithms	32
	F.2	Datase	t, Model, Reward, Evaluation Details	34
	F.3	Hyper	parameters	34
G	Con	iplete E	Experiment Results	35
Н	Valu	e Mode	el Size Ablation	36
T	Lim	itations		37

A PROBLEM SETUP DETAILS

Let x denote a prompt (e.g., a math question), and let y denote a sampled solution of length |y| generated autoregressively from a policy π , i.e., $y \sim \pi(\cdot \mid x)$. We assume a binary reward function $r(x,y) \in \{0,1\}$, where r(x,y) = 1 if the final answer in y is correct and 0 otherwise. Our goal is to learn a parameterized policy π_{θ} that maximizes the expected reward over a dataset \mathcal{D} of prompts:

$$J(\theta) = \mathbb{E}_{x \sim \mathcal{D}, y \sim \pi_{\theta}(\cdot|x)}[r(x,y)]. \tag{4}$$

Following the standard REINFORCE derivation (Williams, 1992), the gradient of this objective can be written as $\nabla_{\theta} J(\theta) = \mathbb{E}_{x,y} [r(x,y)\nabla_{\theta} \log \pi_{\theta}(y \mid x)].$

To reduce the variance of this estimator, it is common to subtract a baseline function that depends only on the prompt x, which does not change the optimum of the policy gradient (Kool et al., 2019; Richter et al., 2020; Zhu et al., 2023; Shao et al., 2024). In this work, we use the expected reward under the current policy, $\mathbb{E}_{y'\sim\pi_{\theta}(\cdot|x)}[r(x,y')]$, as the baseline, which is standard in LLM post-training (Shao et al., 2024; DeepSeek-AI, 2025; Yu et al., 2025; Liu et al., 2025). Since the reward is binary, we define $p_{\pi_{\theta}}(x) \coloneqq \mathbb{E}_{y\sim\pi_{\theta}(\cdot|x)}[r(x,y)]$ as the probability of generating a correct answer, and $A(x,y) \coloneqq r(x,y) - p_{\pi_{\theta}}(x)$ as the advantage. The policy gradient can be expressed as $\nabla_{\theta}J(\theta) = \mathbb{E}_{x\sim\mathcal{D},y\sim\pi_{\theta}(\cdot|x)}[A(x,y)\nabla_{\theta}\log\pi_{\theta}(y\mid x)]$.

In practice, LLMs are trained with multiple updates on generations produced by some old policy $\pi_{\theta_{\text{old}}}$ and the training is often stabilized using techniques such as PPO-style clipping (Schulman et al., 2017; Shao et al., 2024; Xiong et al., 2025). However, we focus on a **purely on-policy** setting, where each gradient step is followed by the collection of fresh rollouts. Specifically, at each iteration t, we perform a single gradient step to maximize:

$$J(\theta) = \mathbb{E}_{x \sim \mathcal{D}, y \sim \pi_{\theta}(\cdot|x)} [A(x, y) \log \pi_{\theta}(y \mid x)]. \tag{5}$$

Note that the above objective has the same gradient as:

$$J(\theta) = \mathbb{E}_{x \sim \mathcal{D}, y \sim \pi_{\theta_t}(\cdot \mid x)} [A(x, y) \frac{\pi_{\theta}(y \mid x)}{\pi_{\theta_t}(y \mid x)}], \tag{6}$$

since we are purely on-policy and π_{θ_t} is the policy before the update and also serves as the sampling distribution.

Given the autoregressive nature of LLMs, we further decompose the objective into a token-level form, treating each token as an individual action:

$$J(\theta) = \mathbb{E}_{x \sim \mathcal{D}, y \sim \pi_{\theta}(\cdot \mid x)} \left[A(x, y) \log \left(\prod_{l=1}^{|y|} \pi_{\theta}(y_l \mid x, y_{< l}) \right) \right]$$
 (7)

$$= \mathbb{E}_{x \sim \mathcal{D}, y \sim \pi_{\theta}(\cdot \mid x)} \left[A(x, y) \sum_{l=1}^{|y|} \log \pi_{\theta}(y_l \mid x, y_{< l}) \right], \tag{8}$$

where y_l denotes the l-th token in the generated sequence. Similarly, the above objective has the same gradient as:

$$J(\theta) = \mathbb{E}_{x \sim \mathcal{D}, y \sim \pi_{\theta_t}(\cdot | x)} \left[A(x, y) \sum_{l=1}^{|y|} \frac{\pi_{\theta}(y_l \mid x, y_{< l})}{\pi_{\theta_t}(y_l \mid x, y_{< l})} \right]. \tag{9}$$

Normalize by the length of y, we arrive at

$$J(\theta) = \mathbb{E}_{x \sim \mathcal{D}, y \sim \pi_{\theta_t}(\cdot|x)} \left[\frac{1}{|y|} A(x, y) \sum_{l=1}^{|y|} \frac{\pi_{\theta}(y_l \mid x, y_{< l})}{\pi_{\theta_t}(y_l \mid x, y_{< l})} \right].$$
 (10)

This objective corresponds to a purely on-policy variant of GRPO (Shao et al., 2024; DeepSeek-AI, 2025), without KL regularization to a fixed reference policy $\pi_{\rm ref}$ (Yu et al., 2025) and without standard deviation-based advantage regularization (Liu et al., 2025). We adopt this formulation to eliminate the off-policyness during updates, clipping heuristics, and additional hyperparameters. This results in a **clean** experimental setup that is directly derived from the original RL objective in Eq. 4.

B RELATED WORK

LLM Post-training. Reinforcement learning (RL) has become a standard for post-training LLMs, including Reinforcement Learning from Human Feedback (RLHF) (Ouyang et al., 2022; Christiano et al., 2023; OpenAI, 2024a; Team, 2025a), enabling the LLMs to generate faithful and harmless responses that closely follow the instruction, and Reinforcement Learning with Verifiable Rewards (RLVR) (OpenAI, 2024b; Yang et al., 2024; DeepSeek-AI, 2025; Qwen, 2025; Lambert et al., 2025; Team, 2025b), improving model reasoning capabilities using verifiable rewards. These methods typically use algorithms include PPO (Schulman et al., 2017), GRPO (Shao et al., 2024), DR-GRPO (Liu et al., 2025), OREO (Wang et al., 2024), DQO (Ji et al., 2024), and VinePPO (Kazemnejad et al., 2025).

Efficient RL for LLM Post-training. Given the huge parameter size for LLMs, there is a large body of work recently focusing on developing more efficient algorithms and data selection methods to enable more efficient RL training for LLMs. Algorithmically, DPO (Rafailov et al., 2024), RAFT (Dong et al., 2023), REBEL (Gao et al., 2024), REFUEL (Gao et al., 2025), A^* -PO (Brantley et al., 2025), RAFT++ (Xiong et al., 2025), RLOO (Ahmadian et al., 2024), and REINFORCE++ (Hu et al., 2025) are all trying to construct new objective functions that either reduces the number of models used (e.g. value model, reference model, reward model) or reduces the number of generations required for online RL. Another line of works (Xia et al., 2024; Muennighoff et al., 2025; Ye et al., 2025; Muldrew et al., 2024; Das et al., 2025; Wang et al., 2025b; Sun et al., 2025; Wang et al., 2025a; Lin et al., 2025) focuses on improving data selections by reducing the amount of training data to be more sample efficient. DAPO (Yu et al., 2025) and VAPO (Yue et al., 2025) resample and keep generating until the effective ratio of the batch is 1 during each step of RL training. However, the generations for a prompt that are either all correct or incorrect are wasted. SPEED (Zhang et al., 2025) improves on top of these methods by using a smaller number of generations to estimate the effective ratio and only generate the rest of the generations if the existing ones are not all correct or incorrect. GRESO (Zheng et al., 2025), on the other hand, avoids rollouts by using a dictionary-based approach and recording the historical average reward for each prompt from the last epoch. However, it would suffer from off-policyness especially when the dataset is large.

Our method is the combination of the best of both worlds where PCL directly avoids costly rollouts and also is on-policy. Our method is closely related to a classic class of machine learning techniques, Curriculum Learning (Bengio et al., 2009). Previous works have explored curriculum learning for LLM post-training (Lee et al., 2024; Wen et al., 2025; Shi et al., 2025) by either training on progressively harder prompts ordered before training or focusing on certain difficulty range on the fly during RL. Our work falls in this group by always focusing on intermediate difficulty prompts for the current policy.

C PRELIMINARY INVESTIGATION DETAILS

C.1 DATASET DETAILS

Table 2: Dataset split, maximum prompt length, and maximum generation length

Dataset	Huggingface Dataset Card	Train - Val	Prompt Length	Generation Length
MATH	DigitalLearningGmbH/MATH-lighteval	7.5k - 5k	1,024	4,096
DeepScaleR	agentica-org/DeepScaleR-Preview-Dataset	40.3k - /	1,024	4,096

Table 3: Model prompt format

Model Family	Prompt Format
Qwen (Base) Llama (Instruct)	{prompt} Let's think step by step and output the final answer within . < begin_of_text >< start_header_id >system< end_header_id >Cutting Knowledge Date: December 2023 Today Date: 26 Jul 2024< eot_id >< start_header_id >user< end_header_id >{prompt} Let's think step by step and output the final answer within . < eot_id >< start_header_id >assistant< end_header_id >

C.2 MODEL DETAILS

We perform **full parameter** training on 8 A100 GPUs using Qwen3-1.7B-Base (model card: Qwen/Qwen3-1.7B-Base), Qwen3-4B-Base (model card: Qwen/Qwen3-4B-Base), Qwen3-8B-Base (model card: Qwen/Qwen3-8B-Base), and Llama3.2-3B-it (model card: meta-llama/Llama-3.2-3B-Instruct).

C.3 REWARD DETAILS

We use a rule-based reward function based on the correctness of the response with math-verify, assigning +1 for correct answers and 0 for incorrect ones or generations that exceed the context length. Recent studies (Chen et al., 2025) have proposed incorporating format-based rules into reward calculations to encourage models to follow specific output formats. However, in our experiments, we observed no significant difference in performance with or without such format-based rewards. Therefore, for simplicity, we exclude them from our implementation.

C.4 EVALUATION DETAILS

Following prior work (Zeng et al., 2025), we evaluate model performance on a suite of standard mathematical reasoning benchmarks, including MATH500 (Hendrycks et al., 2021), Minerva Math (Lewkowycz et al., 2022), and OlympiadBench (He et al., 2024), as well as competition-level benchmarks such as AMC 2023, AIME 2024, and AIME 2025.

For smaller-scale datasets, we report results using the average reward across multiple generations. Specifically, for Minerva Math, we report Avg@4; for AMC 2023, AIME 2024, and AIME 2025, we report Avg@32.

For MATH experiments, we use decoding parameters top_k = 20, temperature = 0.6, and top_p = 0.95. For DeepScaleR experiments, we use top_k = -1 (i.e., disabled), temperature = 0.6, and top_p = 0.95.

C.5 COMPLETE LIST OF EXPERIMENTS

The learning rate for each batch size is tuned on a logarithmic scale using the Qwen3-8B-Base model. For all other models, we adopt the corresponding optimal learning rate found for Qwen3-8B-Base. The complete list of all the experiments is provided below with the chosen learning rate highlighted in **bold**.

Table 4: Complete List of Experiments for Math

		Table 4. Col	ubiere rist o	1 Experime	101	iviatil	
Model	# Prompts (m)	#Generations (n)	Context Length	Num Workers	Engine	Batch Size (b)	LR
	64	16	4096	8	VLLM	1024	1E-6/ 2E-6
	128	16	4096	8	VLLM	2048	1E-6/2E-6/5E-6/1E-5
	256	16	4096	8	VLLM	4096	2E-6/ 4E-6 /8E-6
Qwen3-8B-base	512	16	4096	8	VLLM	8192	4E-6/ 8E-6 /1.6E-5
	1024	16	4096	8	VLLM	16384	4E-6/ 8E-6 /1.6E-5
	2048	16	4096	8	VLLM	32768	4E-6/8E-6/1.6E-5/3.2E-5
	4096	16	4096	8	VLLM	65536	8E-6/1.6E-5/ 3.2E-5 /6.4E-5
	64	16	4096	8	VLLM	1024	2.00E-06
	128	16	4096	8	VLLM	2048	2.00E-06
	256	16	4096	8	VLLM	4096	4.00E-06
Qwen3-4B-base	512	16	4096	8	VLLM	8192	8.00E-06
	1024	16	4096	8	VLLM	16384	8.00E-06
	2048	16	4096	8	VLLM	32768	1.60E-05
	4096	16	4096	8	VLLM	65536	3.20E-05
	64	16	4096	8	VLLM	1024	2.00E-06
	128	16	4096	8	VLLM	2048	2.00E-06
	256	16	4096	8	VLLM	4096	4.00E-06
Qwen3-1.7B-base	512	16	4096	8	VLLM	8192	8.00E-06
	1024	16	4096	8	VLLM	16384	8.00E-06
	2048	16	4096	8	VLLM	32768	1.60E-05
	4096	16	4096	8	VLLM	65536	3.20E-05
	64	16	4096	8	VLLM	1024	2.00E-06
	128	16	4096	8	VLLM	2048	2.00E-06
	256	16	4096	8	VLLM	4096	4.00E-06
Llama3.2-3B-it	512	16	4096	8	VLLM	8192	8.00E-06
	1024	16	4096	8	VLLM	16384	8.00E-06
	2048	16	4096	8	VLLM	32768	8.00E-06
	4096	16	4096	8	VLLM	65536	1.20E-05
	32	32	4096	8	VLLM	1024	2.00E-06
	256	32	4096	8	VLLM	8192	8.00E-06
Owen3-4B-base	2048	32	4096	8	VLLM	65536	3.20E-05
Qwcii3-4D-base	16	64	4096	8	VLLM	1024	2.00E-06
	128	64	4096	8	VLLM	8192	8.00E-06
	1024	64	4096	8	VLLM	65536	3.20E-05

Model	#Prompts (m)	#Generations (n)	Context Length	Num Workers	Engine	Batch Size	LR
	64	16	4096	8	VLLM	1024	1E-6/ 2E-6
	128	16	4096	8	VLLM	2048	1E-6/ 2E-6 /5E-6/1E-5/2E-
	256	16	4096	8	VLLM	4096	2E-6/ 4E-6 /8E-6
Qwen3-8B-base	512	16	4096	8	VLLM	8192	2E-6/ 4E-6 /6E-6
	1024	16	4096	8	VLLM	16384	4E-6/ 8E-6 /1.2E-5/1.6E-5
	2048 4096	16 16	4096 4096	8 8	VLLM VLLM	32768 65536	8E-6/ 1.2E-5 /1.6E-5 8E-6/ 1.2E-5 /1.6E-5
	64	16	4096	8	VLLM	1024	2.00E-06
	128	16	4096	8	VLLM	2048	2.00E-06
	256	16	4096	8	VLLM	4096	4.00E-06
Owen3-4B-base	512	16	4096	8	VLLM	8192	4.00E-06
Queno 12 case	1024	16	4096	8	VLLM	16384	8.00E-06
	2048	16	4096	8	VLLM	32768	1.20E-05
	4096	16	4096	8	VLLM	65536	1.20E-05
	64	16	4096	8	VLLM	1024	2.00E-06
	128	16	4096	8	VLLM	2048	2.00E-06
	256	16	4096	8	VLLM	4096	4.00E-06
Qwen3-1.7B-base	512	16	4096	8	VLLM	8192	4.00E-06
	1024	16	4096	8	VLLM	16384	8.00E-06
	2048	16	4096	8	VLLM	32768	1.20E-05
	4096	16	4096	8	VLLM	65536	1.20E-05
	64	16	4096	8	VLLM	1024	2.00E-06
	128	16	4096	8	VLLM	2048	2.00E-06
	256	16	4096	8	VLLM	4096	4.00E-06
Llama3.2-3B-it	512	16	4096	8	VLLM	8192	4.00E-06
	1024	16	4096	8	VLLM	16384	8.00E-06
	2048 4096	16 16	4096 4096	8 8	VLLM VLLM	32768 65536	8.00E-06 1.20E-05
	32	32	4096	8	VLLM	1024	2.00E-06
	256	32 32	4096 4096	8	VLLM VLLM	8192 65536	4.00E-06
Qwen3-4B-base	2048 16	64	4096	8 8	VLLM	1024	1.20E-05 2.00E-06
	128	64	4096	8	VLLM	8192	4.00E-06
	1024	64	4096	8	VLLM	65536	1.20E-05
	64	16	8192	8	VLLM	1024	2.00E-06
	128	16	8192	8	VLLM	2048	2.00E-06
	256	16	8192	8	VLLM	4096	4.00E-06
Qwen3-4B-base	512	16	8192	8	VLLM	8192	4.00E-06
	1024	16	8192	8	VLLM	16384	8.00E-06
	2048	16	8192	8	VLLM	32768	1.20E-05
	4096	16	8192	8	VLLM	65536	1.20E-05
	16	16	4096	1	VLLM	256	1.00E-06
	32	16	4096	1	VLLM	512	1.00E-06
	64	16	4096	1	VLLM	1024	2.00E-06
Qwen3-4B-base	128	16	4096	1	VLLM	2048	2.00E-06
	256	16	4096	1	VLLM	4096	4.00E-06
	512 1024	16 16	4096 4096	1 1	VLLM VLLM	8192 16384	4.00E-06 8.00E-06
	16	16	4096	8	SGLang	256	1.00E-06
	32 64	16	4096	8 8	SGLang	512	1.00E-06
	128	16 16	4096 4096	8	SGLang SGLang	1024 2048	2.00E-06
Qwen3-4B-base	256	16	4096	8	SGLang	4096	2.00E-06 4.00E-06
Aweno-4p-pase	512	16	4096 4096	8	SGLang	4096 8192	4.00E-06 4.00E-06
					JULANS	0174	T.UUL-UU
					SGI and	16384	8 00E-06
	1024 2048	16 16	4096 4096	8	SGLang SGLang	16384 32768	8.00E-06 1.20E-05

Table	6: Complet	e List of Expe	eriments for I	DeepScaleR	(cont.))	
Model	#Prompts (m)	#Generations (n)	Context Length	Num Workers	Engine	Batch Size	LR
	32	128	4096	8	VLLM	4096	4.00E-06
	64	64	4096	8	VLLM	4096	4.00E-06
	128	32	4096	8	VLLM	4096	4.00E-06
	256	16	4096	8	VLLM	4096	4.00E-06
Qwen3-4B-Base & $p(x) = 0$	512	8	4096	8	VLLM	4096	4.00E-06
	1024	4	4096	8	VLLM	4096	4.00E-06
	2048	2	4096	8	VLLM	4096	4.00E-06
	32	128	4096	8	VLLM	4096	4.00E-06
	64	64	4096	8	VLLM	4096	4.00E-06
	128	32	4096	8	VLLM	4096	4.00E-06
	256	16	4096	8	VLLM	4096	4.00E-06
Qwen3-4B-Base & $p(x) = 0.25$	512	8	4096	8	VLLM	4096	4.00E-06
	1024	4	4096	8	VLLM	4096	4.00E-06
	2048	2	4096	8	VLLM	4096	4.00E-06
	32	128	4096	8	VLLM	4096	4.00E-06
	64	64	4096	8	VLLM	4096	4.00E-06
	128	32	4096	8	VLLM	4096	4.00E-06
	256	16	4096	8	VLLM	4096	4.00E-06
Qwen3-4B-Base & $p(x) = 0.5$	512	8	4096	8	VLLM	4096	4.00E-06
	1024	4	4096	8	VLLM	4096	4.00E-06
	2048	2	4096	8	VLLM	4096	4.00E-06
	32	128	4096	8	VLLM	4096	4.00E-06
	64	64	4096	8	VLLM	4096	4.00E-06
	128	32	4096	8	VLLM	4096	4.00E-06
	256	16	4096	8	VLLM	4096	4.00E-06
Qwen3-4B-Base & $p(x) = 0.75$	512	8	4096	8	VLLM	4096	4.00E-06
	1024	4	4096	8	VLLM	4096	4.00E-06
	2048	2	4096	8	VLLM	4096	4.00E-06
	32	128	4096	8	VLLM	4096	4.00E-06
	64	64	4096	8	VLLM	4096	4.00E-06
	128	32	4096	8	VLLM	4096	4.00E-06
	256	16	4096	8	VLLM	4096	4.00E-06
Qwen3-4B-Base & $p(x) = 1$	512	8	4096	8	VLLM	4096	4.00E-06
• •	1024	4	4096	8	VLLM	4096	4.00E-06
	2048	2	4096	8	VLLM	4096	4.00E-06

D PRELIMINARY INVESTIGATION COMPLETE RESULTS

D.1 Complete Results for Section 3.1

D.1.1 RESULTS WITH VARYING m

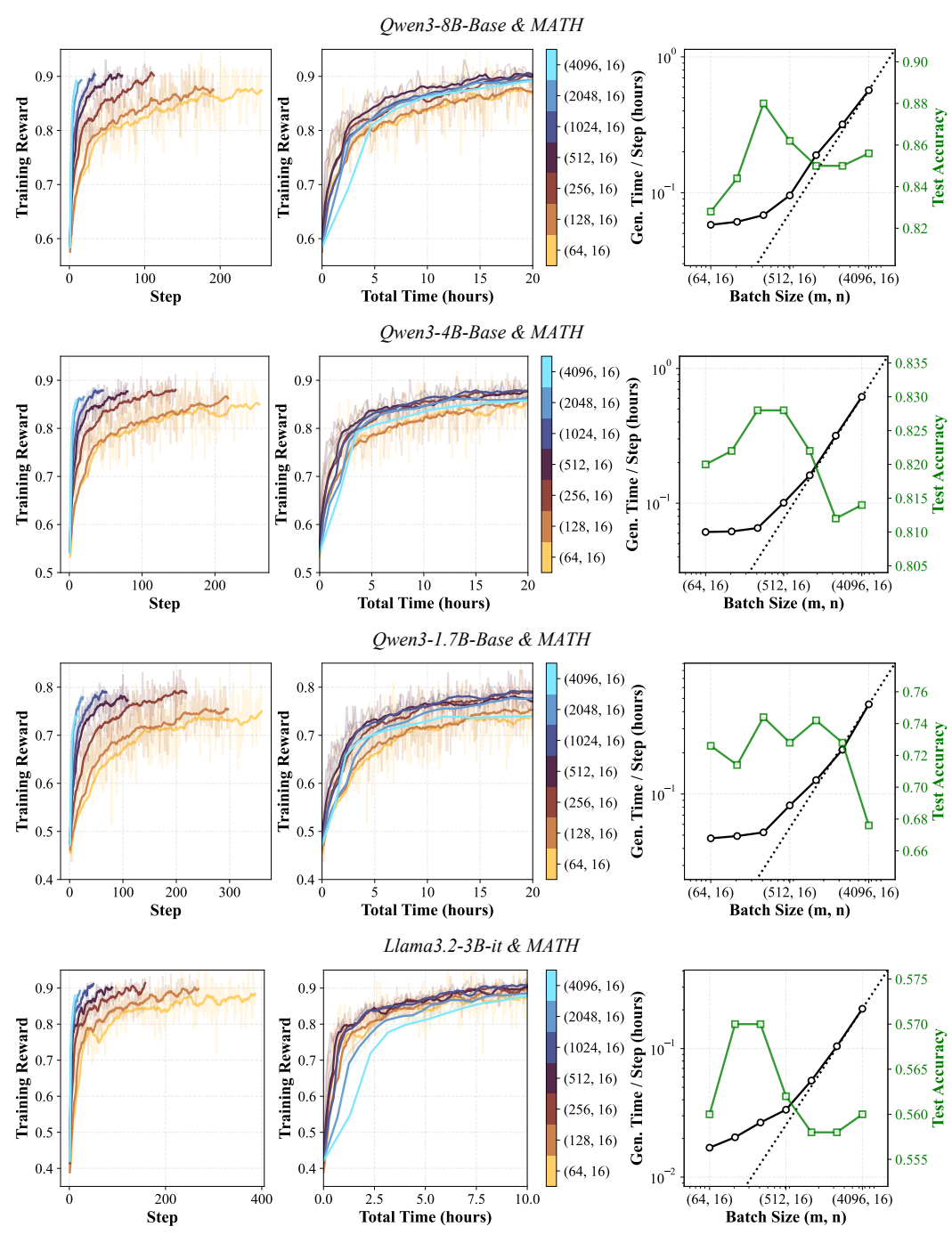


Figure 10: Results for all four models on MATH with n=16. (Left / Middle) Training reward as a function of training steps and wall-clock time. The legend indicates the batch configuration in terms of (number of prompts m, generations per prompt n). (Right) Generation time per step and test accuracy across different batch sizes. The dashed line represents the linear increase that intercepts the origin and the generation time for the largest batch size. Both axes are in log scale.

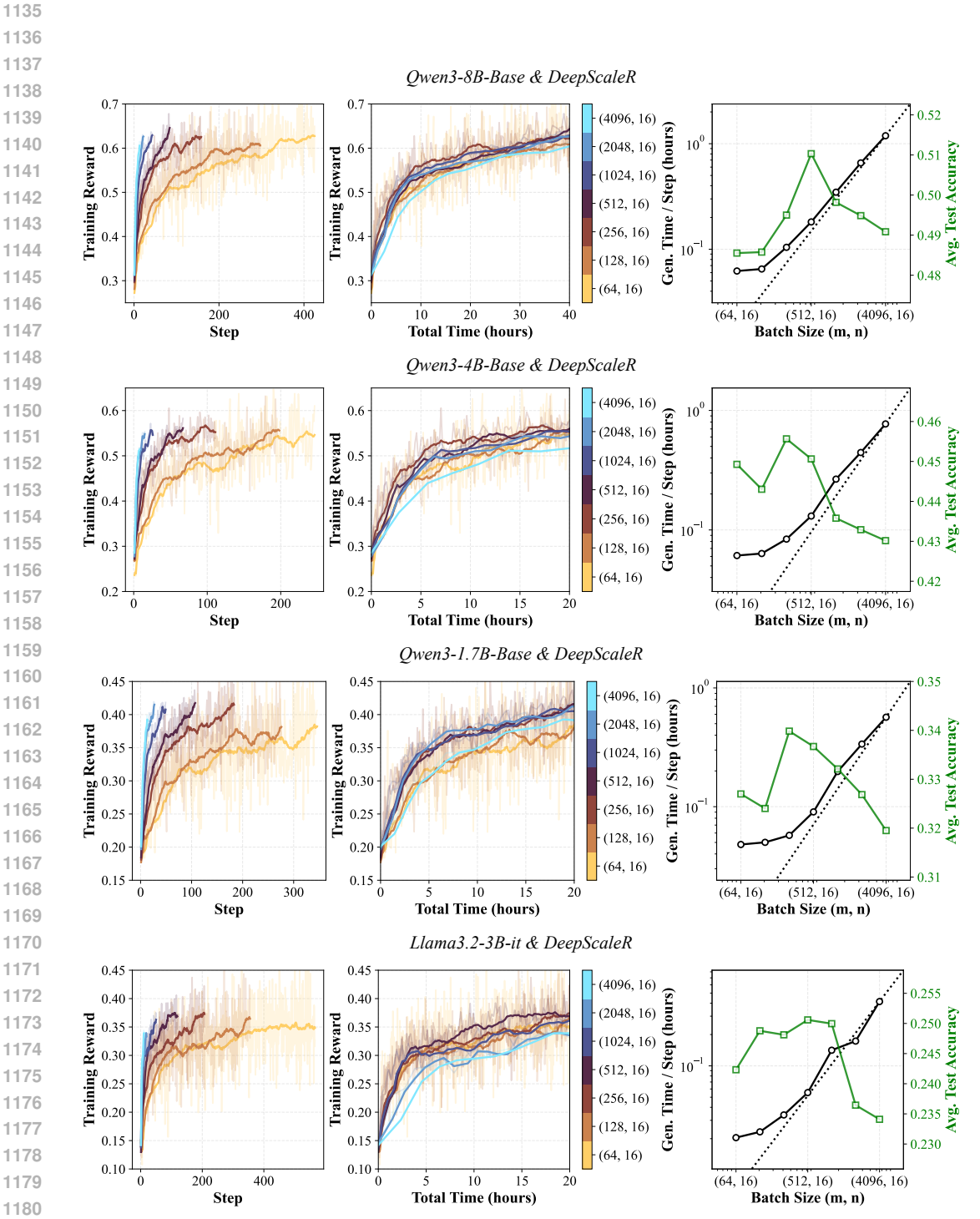


Figure 11: Results for all four models on DeepScaleR with n = 16. (Left / Middle) Training reward as a function of training steps and wall-clock time. The legend indicates the batch configuration in terms of (number of prompts m, generations per prompt n). (Right) Generation time per step and test accuracy across different batch sizes. The dashed line represents the linear increase that intercepts the origin and the generation time for the largest batch size. Both axes are in log scale.

Table 7: Detailed Results for Fig. 11.

Model	m	MATH500	Olymp.	Minerva Avg@4	AMC23 Avg@32	AIME24 Avg@32	AIME25 Avg@32	Avg.
	π_{ref}	70.2	34.3	29.8	49.1	15.8	8.8	34.7
	4096	85.8	52.2	43.0	70.9	21.5	21.1	49.1
	2048	85.2	53.4	43.9	66.6	26.4	21.5	49.5
O2 OD D	1024	85.6	54.9	45.9	70.5	22.8	19.3	49.8
Qwen3-8B-Base	512	87.2	55.8	44.1	71.8	26.1	21.1	51.0
	256	85.0	57.4	40.4	66.3	24.9	22.9	49.5
	128	85.6	53.9	42.0	67.8	22.3	19.9	48.6
	64	85.2	54.7	42.1	70.6	21.4	17.3	48.6
	π_{ref}	65.8	34.4	26.9	47.3	10.9	7.1	32.1
	4096	80.6	45.8	39.7	59.8	16.4	15.8	43.0
	2048	83.2	48.4	39.2	57.0	16.0	15.9	43.3
Owen 2 4D Daga	1024	81.6	46.1	40.2	59.3	18.1	16.1	43.6
Qwen3-4B-Base	512	84.0	49.7	38.8	62.9	17.1	17.9	45.1
	256	82.8	48.1	40.3	66.3	17.8	18.1	45.6
	128	83.8	46.0	42.6	59.5	18.2	15.6	44.3
	64	83.2	48.2	39.7	64.1	17.6	16.8	44.9
	π_{ref}	57.0	23.9	21.8	29.0	3.8	1.1	22.8
	4096	69.8	35.2	29.0	40.7	9.1	8.0	32.0
	2048	70.2	34.3	31.2	42.0	12.2	6.2	32.7
Owen 2 1 7D Dags	1024	72.2	36.2	29.7	41.8	12.4	7.0	33.2
Qwen3-1.7B-Base	512	71.8	37.1	30.1	44.2	12.7	6.1	33.7
	256	72.6	35.6	31.5	46.9	10.1	7.2	34.0
	128	68.4	35.2	30.0	43.3	10.9	6.7	32.4
	64	70.2	36.5	30.0	40.8	11.2	7.5	32.7
	π_{ref}	42.8	12.3	13.8	19.7	4.6	0.4	15.6
	4096	55.2	20.0	21.1	31.6	11.9	0.6	23.4
	2048	55.8	19.3	21.2	30.9	13.8	0.9	23.6
Llama3.2-3B-it	1024	57.8	22.8	21.2	34.8	12.1	1.2	25.0
Liama3.2-3D-II	512	58.0	22.3	22.7	30.0	15.8	1.6	25.1
	256	57.6	21.8	22.6	32.0	14.5	0.4	24.8
	128	55.6	22.7	22.2	34.8	13.9	0.1	24.9
	64	56.8	20.9	25.5	31.8	10.2	0.2	24.2

D.1.2 RESULTS WITH VARYING m AND n

Table 8: Detailed DeepScaleR Results for Fig. 12.

Model	m	n	MATH500	Olymp.	Minerva Avg@4	AMC23 Avg@32	AIME24 Avg@32	AIME25 Avg@32	Avg.
	π_{ref}		65.8	34.4	26.9	47.3	10.9	7.1	32.1
	32	32	80.4	47.5	37.4	57.4	17.5	14.4	42.4
	256	32	83.2	49.1	38.6	63.4	17.3	16.0	44.6
Qwen3-4B-Base	2048	32	81.4	46.3	39.8	57.6	17.6	15.5	43.0
Qwell3-4b-base	16	64	81.6	47.8	39.2	58.4	15.7	14.3	42.8
	128	64	83.4	44.4	41.5	60.0	17.0	13.1	43.2
	1024	64	80.8	48.7	39.2	57.0	16.4	13.8	42.6

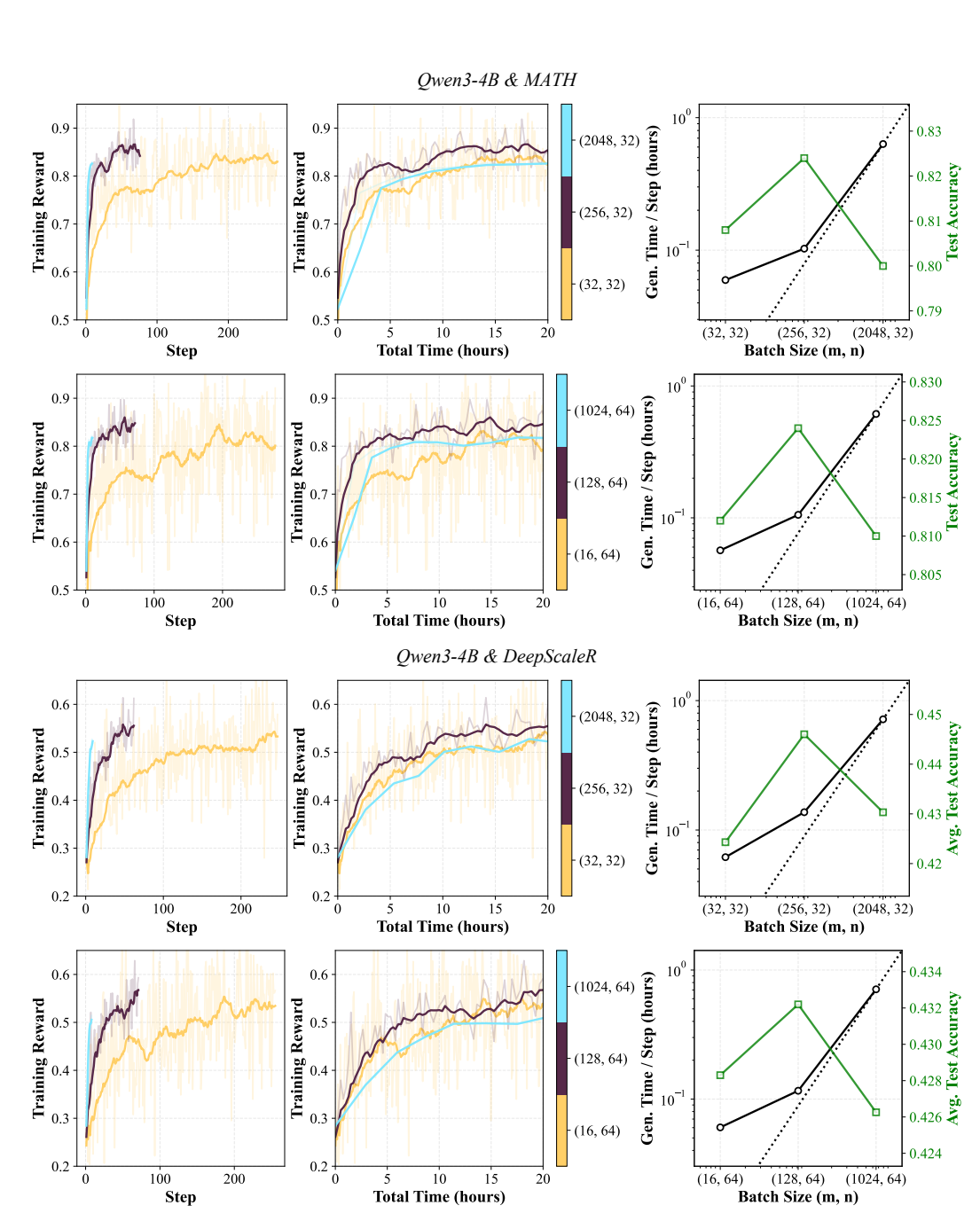


Figure 12: Results for Qwen3-4B on MATH and DeepScaleR with n=32 and 64. (Left / Middle) Training reward as a function of training steps and wall-clock time. The legend indicates the batch configuration in terms of (number of prompts m, generations per prompt n). (Right) Generation time per step and test accuracy across different batch sizes. The dashed line represents the linear increase that intercepts the origin and the generation time for the largest batch size. Both axes are in log scale.

D.1.3 RESULTS WITH A DIFFERENT CONTEXT LENGTH

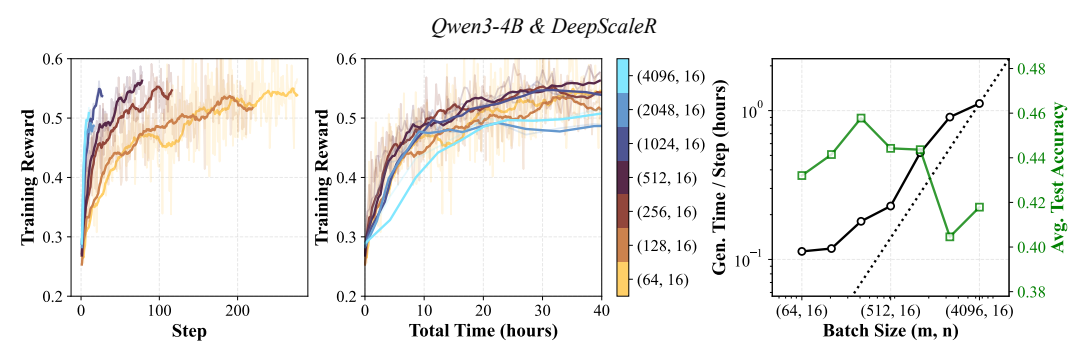


Figure 13: Results for Qwen3-4B on DeepScaleR with context length 8192 (other results are using 4096 context length). (Left / Middle) Training reward as a function of training steps and wall-clock time. The legend indicates the batch configuration in terms of (number of prompts m, generations per prompt n). (Right) Generation time per step and test accuracy across different batch sizes. The dashed line represents the linear increase that intercepts the origin and the generation time for the largest batch size. Both axes are in log scale.

Table 9: Detailed DeepScaleR Results for Fig. 13.

Model	m	Context Len.	MATH500	Olymp.	Minerva Avg@4	AMC23 Avg@32	AIME24 Avg@32	AIME25 Avg@32	Avg.
	π_{ref}		65.8	34.4	26.9	47.3	10.9	7.1	32.1
	64	8K	80.4	47.9	39.2	60.7	15.9	15.1	43.2
	128	8K	83.0	50.6	38.4	62.3	14.2	16.4	44.1
Orrigan 2 AD Dogg	256	8K	82.8	50.4	42.2	62.0	19.3	18.0	45.8
Qwen3-4B-Base	512	8K	81.2	49.6	41.0	65.3	17.0	12.5	44.4
	1024	8K	80.8	46.6	39.7	63.7	16.6	18.9	44.4
	2048	8K	77.6	44.4	37.5	54.5	14.2	14.6	40.5
	4096	8K	79.8	45.3	38.9	58.4	14.7	13.8	41.8

D.1.4 RESULTS WITH A DIFFERENT HARDWARE CONFIGURATION

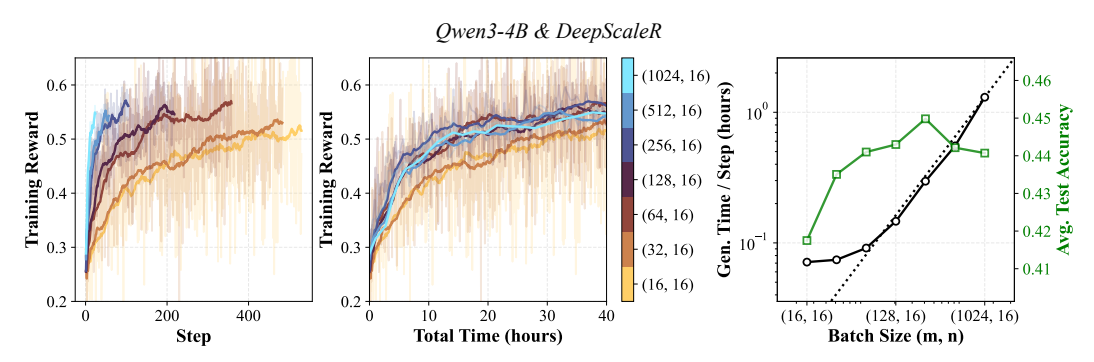


Figure 14: Results for Qwen3-4B on DeepScaleR with only 1 rollout worker with 8 GPUs (other results are using 8 rollout workers, 1 per GPU). (Left / Middle) Training reward as a function of training steps and wall-clock time. The legend indicates the batch configuration in terms of (number of prompts m, generations per prompt n). (Right) Generation time per step and test accuracy across different batch sizes. The dashed line represents the linear increase that intercepts the origin and the generation time for the largest batch size. Both axes are in log scale.

Table 10: Detailed DeepScaleR Results for Fig. 14.

Model	m	Num. Worker	MATH500	Olymp.	Minerva Avg@4	AMC23 Avg@32	AIME24 Avg@32	AIME25 Avg@32	Avg.
	π_{ref}		65.8	34.4	26.9	47.3	10.9	7.1	32.1
	16	1	78.4	47.2	39.2	58.0	15.3	12.4	41.7
	32	1	81.8	47.0	39.0	61.3	17.1	14.9	43.5
Owen 2 4D Door	64	1	83.6	49.4	40.6	58.7	15.9	16.4	44.1
Qwen3-4B-Base	128	1	82.4	48.7	39.2	62.7	17.2	15.7	44.3
	256	1	82.8	49.6	38.6	62.6	18.9	17.5	45.0
	512	1	81.6	47.6	40.7	62.1	17.7	15.5	44.2
	1024	1	80.4	47.8	40.4	60.1	18.9	16.9	44.1

D.1.5 RESULTS WITH A DIFFERENT INFERENCE ENGINE

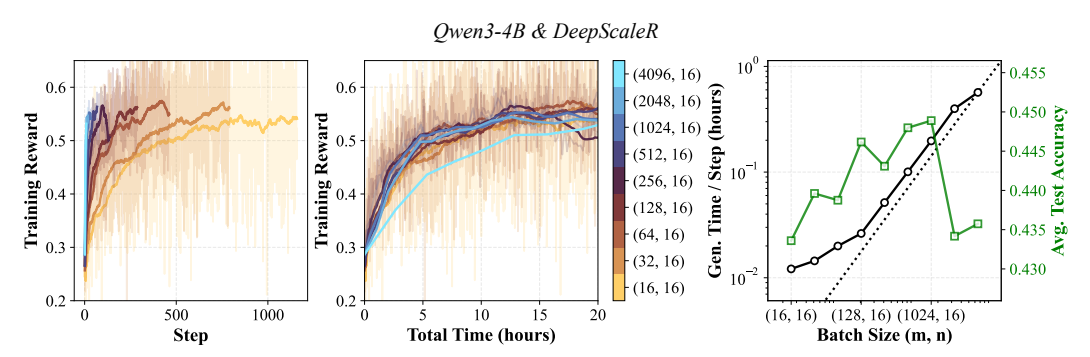


Figure 15: Results for Qwen3-4B on DeepScaleR with SGLang (other results are using VLLM). (Left / Middle) Training reward as a function of training steps and wall-clock time. The legend indicates the batch configuration in terms of (number of prompts m, generations per prompt n). (Right) Generation time per step and test accuracy across different batch sizes. The dashed line represents the linear increase that intercepts the origin and the generation time for the largest batch size. Both axes are in log scale.

Table 11: Detailed DeepScaleR Results for Fig. 15.

Model	m	Inference Eng.	MATH500	Olymp.	Minerva Avg@4	AMC23 Avg@32	AIME24 Avg@32	AIME25 Avg@32	Avg.
	π_{ref}		65.8	34.4	26.9	47.3	10.9	7.1	32.1
	16	SGLang	81.8	48.5	37.3	58.0	17.1	17.4	43.4
Qwen3-4B-Base	32	SGLang	81.2	49.9	40.0	60.9	17.0	14.9	44.0
	64	SGLang	81.6	50.9	39.8	60.2	15.3	15.4	43.9
	128	SGLang	84.0	48.8	39.7	62.9	15.2	17.1	44.6
	256	SGLang	81.8	49.4	40.0	60.4	16.6	17.7	44.3
	512	SGLang	82.2	50.3	40.9	63.2	17.0	15.2	44.8
	1024	SGLang	81.2	51.3	41.0	62.9	16.8	16.1	44.9
	2048	SGLang	81.2	46.0	40.6	61.0	17.3	14.4	43.4
	4096	SGLang	82.0	47.8	39.8	61.9	16.2	13.8	43.6

D.2 Complete Results for Section 3.2

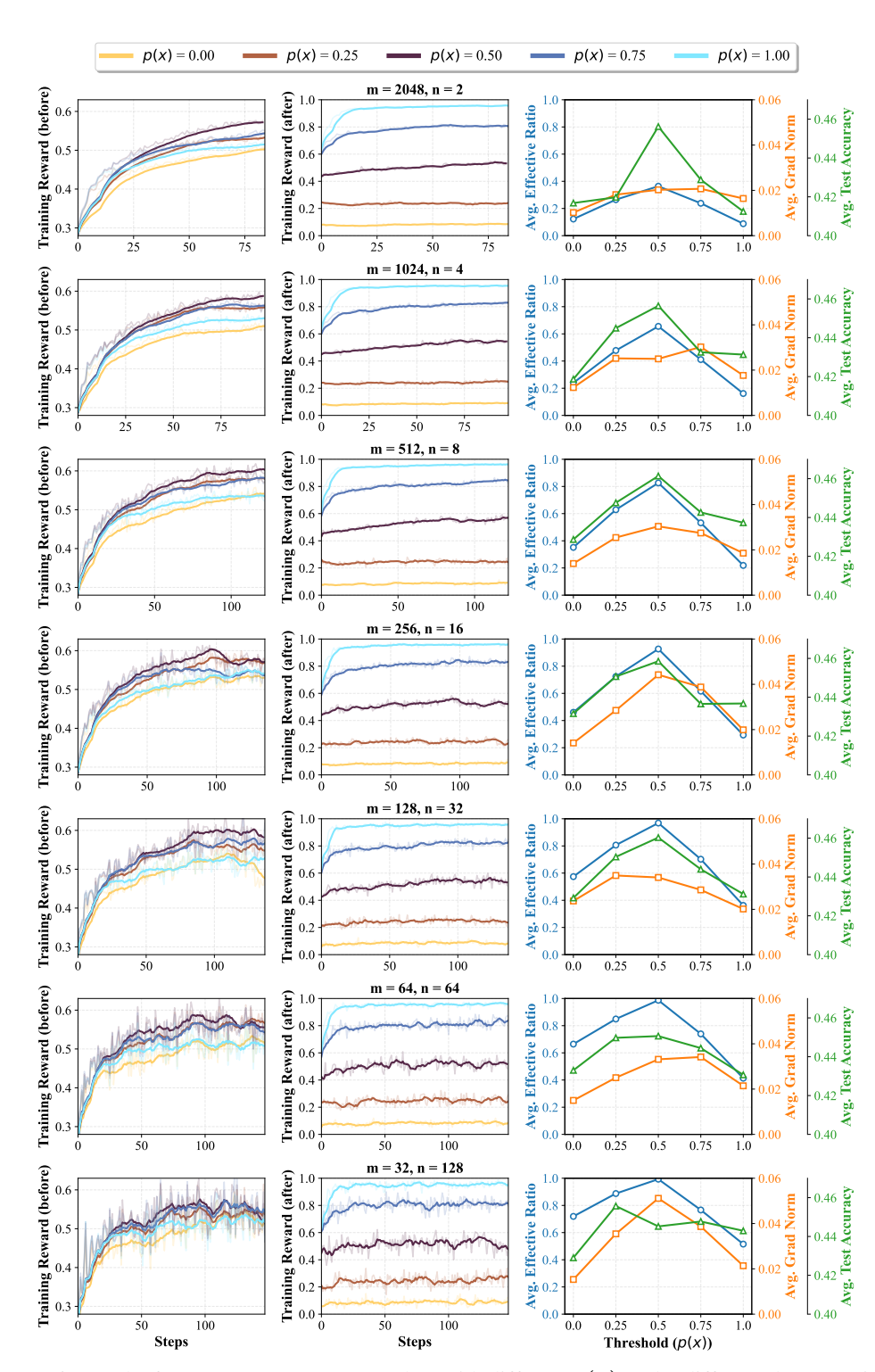


Figure 16: Results for Qwen3-4B on DeepScaleR with different p(x) under different decompositions, grouped by number of prompts m and generations per prompt n. (Left) Training reward before downsampling in terms of step. (Middle) Training reward after downsampling. (Right) Average effective ratio, gradient norm, and test accuracy across different thresholds.

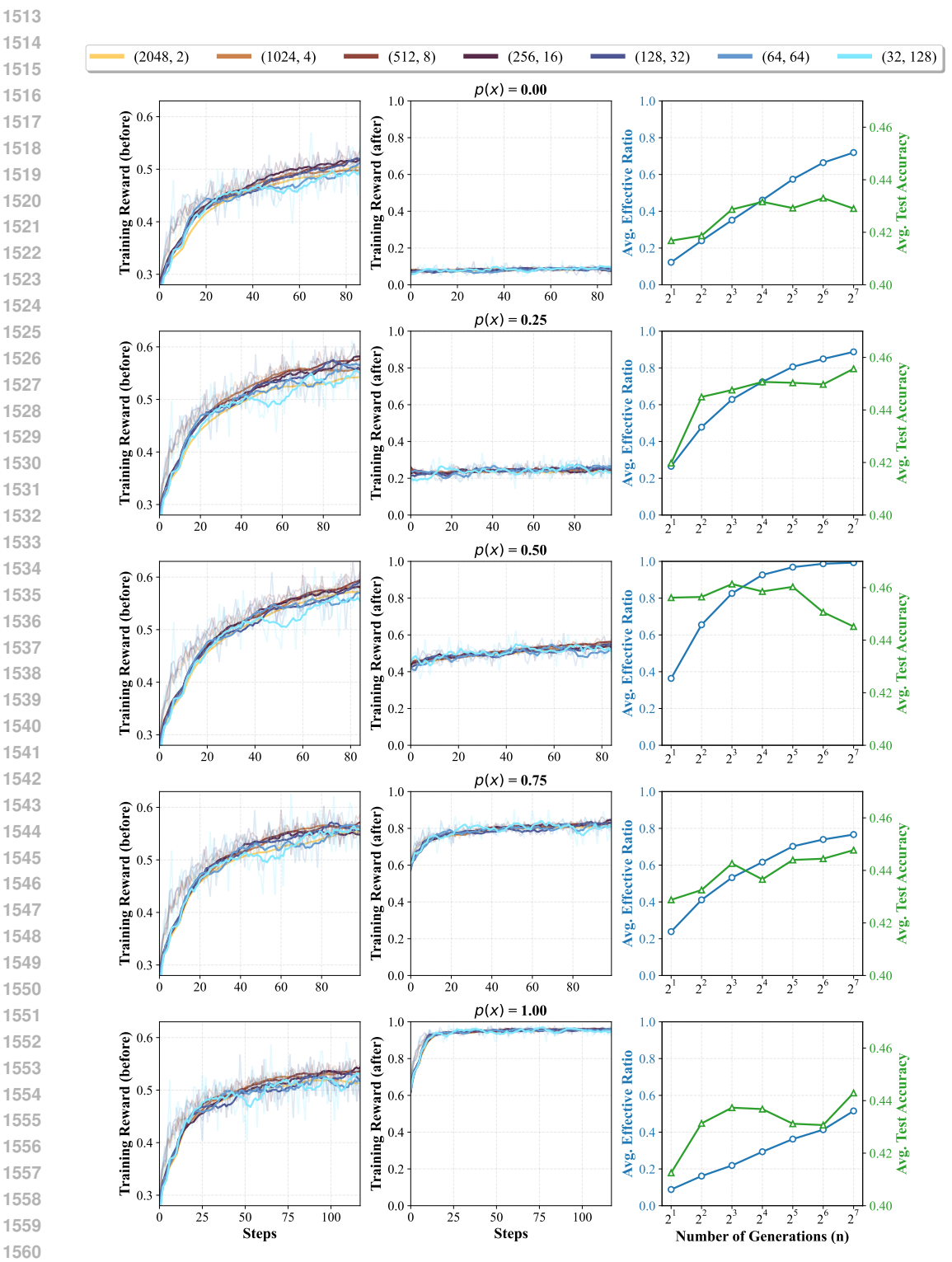


Figure 17: Results for Qwen3-4B on DeepScaleR with different p(x) under different decompositions (number of prompts m, generations per prompt n), grouped by p(x). (Left) Training reward before downsampling in terms of step. (Middle) Training reward after downsampling. (Right) Average effective ratio, gradient norm, and test accuracy across different thresholds.

Table 12: Detailed DeepScaleR Results for Fig. 16 and 17.

p(x)	m	n	MATH500	Olymp.	Minerva Avg@4	AMC23 Avg@32	AIME24 Avg@32	AIME25 Avg@32	Avg.
/	π_{ref}		65.8	34.4	26.9	47.3	10.9	7.1	32.1
0	2048	2	82.8	44.8	39.4	54.3	15.3	13.4	41.7
	1024	4	81.8	44.7	38.4	54.8	17.1	14.5	41.9
	512	8	82.6	48.1	40.0	57.5	14.7	14.4	42.9
	256	16	83.4	46.6	39.4	58.0	16.7	14.9	43.2
	128	32	79.8	45.1	38.1	59.4	18.2	16.9	42.9
	64	64	83.4	47.3	40.7	59.3	15.4	13.6	43.3
	32	128	81.0	49.1	38.5	54.8	17.7	16.2	42.9
	2048	2	80.6	46.9	39.4	58.3	15.5	11.1	42.0
	1024	4	84.2	48.2	39.9	61.6	16.6	16.5	44.5
	512	8	81.8	49.3	40.1	61.2	20.7	15.5	44.8
0.25	256	16	82.8	47.0	38.5	63.2	19.6	19.3	45.1
	128	32	81.0	50.1	40.1	63.0	21.6	14.4	45.0
	64	64	83.4	49.1	41.6	58.8	19.1	17.8	45.0
	32	128	84.0	49.1	40.0	61.9	19.5	19.0	45.6
	2048	2	83.2	50.7	40.0	60.9	19.2	19.7	45.6
	1024	4	81.4	53.7	40.5	63.7	17.2	17.3	45.6
	512	8	84.2	50.1	40.3	64.6	21.5	16.1	46.1
0.5	256	16	82.8	49.7	41.5	62.4	19.5	19.3	45.9
	128	32	84.4	51.8	39.8	64.4	20.1	15.7	46.0
	64	64	83.6	48.8	39.4	61.9	19.9	16.8	45.1
	32	128	81.6	45.7	40.8	62.0	20.1	16.9	44.5
	2048	2	81.0	48.7	39.0	56.6	17.5	14.6	42.9
	1024	4	82.0	49.7	38.6	58.3	16.5	14.5	43.3
0.75	512	8	81.6	47.6	40.6	60.9	16.6	18.2	44.3
	256	16	81.4	46.1	39.1	64.0	17.2	14.2	43.7
	128	32	81.6	50.0	40.3	63.6	15.0	15.9	44.4
	64	64	81.0	50.0	41.1	61.9	15.1	17.6	44.4
	32	128	82.0	49.3	40.6	62.0	17.7	17.1	44.8
	2048	2	78.6	46.6	41.6	55.8	14.3	10.6	41.3
1	1024	4	80.8	48.8	38.3	60.2	16.7	14.0	43.1
	512	8	82.4	45.7	39.9	59.0	18.8	16.7	43.7
	256	16	82.0	46.7	40.6	58.8	18.4	15.5	43.7
	128	32	81.4	48.2	39.3	57.6	17.0	15.2	43.1
	64	64	81.2	46.9	40.7	56.8	18.8	14.1	43.1
	32	128	82.4	45.5	39.7	62.9	16.6	18.6	44.3

E CONNECTION BETWEEN p(x) AND GRADIENT MAGNITUDE

We now analyze the squared norm of the gradient in Eq. (6):

$$\|\nabla_{\theta} J_x(\theta)\|_2 = \|\mathbb{E}_{y \sim \pi_{\theta}(\cdot|x)} [A(x,y)\nabla_{\theta} \log \pi_{\theta}(y|x)]\|_2. \tag{11}$$

Using Jensen inequality, we have:

$$\|\mathbb{E}_{y \sim \pi_{\theta}(\cdot|x)}[A(x,y)\nabla_{\theta}\log \pi_{\theta}(y|x)]\|_{2} \leq \mathbb{E}_{y \sim \pi_{\theta}(\cdot|x)}[\|A(x,y)\nabla_{\theta}\log \pi_{\theta}(y|x)\|_{2}]$$
(12)

$$= \mathbb{E}_{y \sim \pi_{\theta}(\cdot|x)}[|A(x,y)| ||\nabla_{\theta} \log \pi_{\theta}(y|x)||_{2}]. \tag{13}$$

Apply Cauchy-Schwarz:

$$\mathbb{E}_{y \sim \pi_{\theta}(\cdot|x)}[|A(x,y)| \, ||\nabla_{\theta} \log \pi_{\theta}(y|x)||_{2}] \leq \sqrt{\mathbb{E}_{y \sim \pi_{\theta}(\cdot|x)}[A(x,y)^{2}]} \sqrt{\mathbb{E}_{y \sim \pi_{\theta}(\cdot|x)}[||\nabla_{\theta} \log \pi_{\theta}(y|x)||_{2}^{2}]}.$$
(14)

Now let's derive for $\mathbb{E}_{y \sim \pi_{\theta}(\cdot|x)}[A(x,y)^2]$:

$$\mathbb{E}_{y \sim \pi_{\theta}(\cdot|x)}[A(x,y)^{2}] = \mathbb{E}_{y \sim \pi_{\theta}(\cdot|x)}[(r(x,y) - p_{\pi_{\theta}}(x))^{2}]$$
(15)

$$= p_{\pi_{\theta}}(x)(1 - p_{\pi_{\theta}}(x))^{2} + (1 - p_{\pi_{\theta}}(x))(0 - p_{\pi_{\theta}}(x))^{2}$$
 (16)

$$= p_{\pi_{\theta}}(x)(1 - p_{\pi_{\theta}}(x)) \tag{17}$$

which is maximized at $p_{\pi_{\theta}}(x) = \frac{1}{2}$. Therefore, intermediate-level prompts yield the largest expected magnitude of advantage and upper bound on gradient updates. These observations motivate a prompt curriculum strategy that prioritizes prompts with intermediate difficulty $(p_{\pi_{\theta}}(x) = \frac{1}{2})$ to enhance training efficiency.

EXPERIMENT DETAILS

BASELINES ALGORITHMS F.1

We list the pseudo-code for GRPO, Pre-filter, DS, and SPEED. For the pseudo-code of GRESO, please refer to Zheng et al. (2025).

Algorithm 2 GRPO

1674

1675 1676

1677

1678

1679

1681

1682 1683

1685

1687

1689

1693

1695

1698 1699

1700

1701

1702 1703

1704

1705

1707

1708

1709

1712

1714 1715

1716 1717 1718

1719

1720

1722 1723 1724

1726 1727 **Require:** Number of prompts m, generations per prompt n

- 1: Initialize policy π_0
- 2: **for** t = 0 to T 1 **do** 1684
 - Sample a batch with m prompts: $\mathcal{D}_m = \{x^i\}_{i=1}^m \subset \mathcal{D}$. 3:
 - Generate n responses: $\mathcal{D}_m = \left\{ (x^i, \{y^{i,j}\}_{j=1}^n) \right\}_{i=1}^m$ where $y^{i,j} \stackrel{\text{iid}}{\sim} \pi_t(\cdot \mid x^i)$. 4:
 - Update to π_{t+1} with GRPO objective using \mathcal{D}_m .
 - 6: end for

Algorithm 3 Pre-filter

Require: Number of prompts m, generations per prompt n, pre-filter generations n_{pre} , thresholds p_{low} and p_{high}

- 1: Initialize policy π_0
- 2: Generate n_{pre} responses for each prompt in the dataset: $\{y^j\}_{j=1}^{n_{\text{pre}}} \sim \pi_0(\cdot|x)$ for each $x \in \mathcal{D}$
- 3: Filter to keep prompts with accuracy between p_{low} and p_{high} :

$$\mathcal{D} \leftarrow \left\{ x \in \mathcal{D} \mid p_{low} < \frac{1}{n_{pre}} \sum_{j=1}^{n_{pre}} r(x, y^j) < p_{high} \right\}$$

- 4: **for** t = 0 to T 1 **do**
- Sample a batch with m prompts: $\mathcal{D}_m = \{x^i\}_{i=1}^m \subset \mathcal{D}$.
- Generate n responses: $\mathcal{D}_m = \left\{ (x^i, \{y^{i,j}\}_{j=1}^n) \right\}_{i=1}^m$ where $y^{i,j} \stackrel{\text{iid}}{\sim} \pi_t(\cdot \mid x^i)$.
- 7: Update to π_{t+1} with GRPO objective using \mathcal{D}_m .
- 8: end for

Algorithm 4 Dynamic-sampling (DS)

Require: Number of prompts m, generations per prompt n, sampling parameter k

- 1: Initialize policy π_0 , $\mathcal{D}_{buffer} \leftarrow \emptyset$
- 2: **for** t = 0 to T 1 **do**
- 3: while $|\mathcal{D}_{\text{buffer}}| < m$ do 1711
 - 4:
- Sample a batch with km prompts: $\mathcal{D}_{km} = \{x^i\}_{i=1}^{km} \subset \mathcal{D}$. Generate n responses: $\mathcal{D}_{km} = \{(x^i, \{y^{i,j}\}_{j=1}^n)\}_{i=1}^{km}$ where $y^{i,j} \stackrel{\text{iid}}{\sim} \pi_t(\cdot \mid x^i)$ Select prompts with mean reward between 0 and 1: 5: 1713

$$\mathcal{D}_{\text{buffer}} \leftarrow \mathcal{D}_{\text{buffer}} \cup \{ (x, \{y^j\}_{j=1}^n) \in \mathcal{D}_{km} \mid 0 < \frac{1}{n} \sum_{j=1}^n r(x, y^j) < 1 \}$$

- 7: end while
 - Sample a batch with m prompts: $\mathcal{D}_m = \{(x^i, \{y^{i,j}\}_{i=1}^n)\}_{i=1}^m \subset \mathcal{D}_{buffer}$. 8:
- $\mathcal{D}_{\text{buffer}} \leftarrow \emptyset$
- 10: Update to π_{t+1} with GRPO objective using \mathcal{D}_m .
- 11: **end for**

Algorithm 5 SPEED Require: Number of prompts m, generations per prompt n, sampling parameter k, screening number of responses n_{init} $(n \ge n_{\text{init}})$ 1: Initialize policy π_0 , $\mathcal{D}_{buffer} \leftarrow \emptyset$, $\mathcal{D}_{accepted} \leftarrow \emptyset$ 2: **for** t = 0 to T - 1 **do** while $|\mathcal{D}_{\text{buffer}}| < m \text{ do}$ 3: Sample a batch with km prompts: $\mathcal{D}_{km} = \{x^i\}_{i=1}^{km} \subset \mathcal{D}$. Generate n_{init} times for \mathcal{D}_{km} and $n-n_{\text{init}}$ times for $\mathcal{D}_{\text{accepted}}$: $\mathcal{D}_{km} = \left\{ (x^i, \{y^{i,j}\}_{j=1}^{n_{\text{init}}}) \right\}_{i=1}^{km} \text{ where } y^{i,j} \overset{\text{iid}}{\sim} \pi_t(\cdot \mid x^i)$ 4: 5: $\mathcal{D}_{\text{accepted}} \leftarrow \mathcal{D}_{\text{accepted}} \cup \left\{ (x^i, \{y^{i,j}\}_{j=1}^{n-n_{\text{init}}}) \right\}_{i=1}^{|\mathcal{D}_{\text{accepted}}|} \text{ where } y^{i,j} \stackrel{\text{iid}}{\sim} \pi_t(\cdot \mid x^i).$ Add $\mathcal{D}_{\text{accepted}}$ to $\mathcal{D}_{\text{buffer}} \cdot \mathcal{D}_{\text{buffer}} \cup \mathcal{D}_{\text{accepted}}$ Select prompts with mean reward between $\mathcal{D}_{\text{accepted}}$ 6: Select prompts with mean reward between 0 and 1 and add to $\mathcal{D}_{accepted}$: $\mathcal{D}_{\text{accepted}} \leftarrow \{ (x, \{y^j\}_{j=1}^{n_{\text{init}}}) \in \mathcal{D}_{km} \mid 0 < \frac{1}{n_{\text{init}}} \sum_{j=1}^{n_{\text{init}}} r(x, y^j) < 1 \}$ end while 8: Sample a batch with m prompts: $\mathcal{D}_m = \left\{ (x^i, \{y^{i,j}\}_{j=1}^n) \right\}_{i=1}^m \subset \mathcal{D}_{\text{buffer}}$. 9: 10: $\mathcal{D}_{\text{buffer}} \leftarrow \mathcal{D}_{\text{buffer}} \setminus \mathcal{D}_{m}$ Update to π_{t+1} with GRPO objective using \mathcal{D}_m . 11: **12: end for**

F.2 DATASET, MODEL, REWARD, EVALUATION DETAILS

We adopt the exact same setting in our preliminary investigation. Refer to Appendix C for details on datasets, models, rewards, and evaluations.

F.3 HYPERPARAMETERS

We list the hyperparameters for each method below. We tune the sample batch size / sampling parameter for DS, SPEED, GRESO, and PCL with the **bolded** one as the best one. For PCL, we always use the same-sized model as the value model for the main results. The learning rate of the value model in PCL is tuned within $\{1e-6, 3e-6, 1e-5\}$. All learning rates make the value model converge to the same performance but larger learning rates are more unstable than the smaller one. Therefore, we pick 1e-6 as the learning rate for the value model. We also tune the sampling parameter k from $\{2,4,8\}$ and observe that it has a minor effect on the accuracy of the value model. Larger values of k lead to higher effective ratios, as the filtering becomes more aggressive. However, increasing k beyond 4 yields only marginal improvements in the effective ratio. Therefore, we set k=4 for all experiments on PCL. An ablation on the value model size is included in Appendix H.

Dataset	Method	Parameters	
MATH	GRPO	m = 512 $lr = 8e - 6$	n = 16
DeepScaleR	GRPO	m = 512 $lr = 4e - 6$	n = 16
MATH	Pre-filter	$m = 512$ $lr = 8e - 6$ $p_{low} = 0$	$n=16$ $n_{ m pre}=16$ $p_{ m high}=1$
DeepScaleR	Pre-filter	$m = 512$ $lr = 4e - 6$ $p_{\text{low}} = 0$	n = 16 n_{pre} = 16 p_{high} = 1
MATH	DS	m = 512 $lr = 8e - 6$	n = 16 $k = 1/2/4$
DeepScaleR	DS	m = 512 $lr = 4e - 6$	n = 16 $k = 1/2/4$
MATH	SPEED	$m = 512$ $lr = 8e - 6$ $n_{\text{init}} = 4/8$	n = 16 $k = 1/2/4$
DeepScaleR	SPEED	$m = 512$ $lr = 4e - 6$ $n_{\text{init}} = 4/8$	n = 16 $k = 1/2/4$
MATH	GRESO	$m = 512$ $lr = 8e - 6$ $p_{easy} = 0.5$ $\alpha_{easy} = 0.083$ $\Delta p = 0.01$	$n = 16$ $B_{\rm r}^{\rm default} = 768/1024$ $p_{hard} = 0.5$ $\alpha_{hard} = 0.167$
DeepScaleR	GRESO	$m = 512$ $lr = 4e - 6$ $p_{easy} = 0.5$ $\alpha_{easy} = 0.083$ $\Delta p = 0.01$	$n = 16$ $B_{\rm r}^{\rm default} = 768/1024$ $p_{hard} = 0.5$ $\alpha_{hard} = 0.167$
MATH	PCL	$m = 512$ $lr = 8e - 6$ $\tau = 0.5$	$n=16$ $lr_{ m critic}=$ 1e-6 /3e-6/1e-5 $k=2/4/8$
DeepScaleR	PCL	$m = 512$ $lr = 4e - 6$ $\tau = 0.5$	$n=16$ $lr_{ m critic}=$ 1e-6 /3e-6/1e-5 $k=2/4/8$

G COMPLETE EXPERIMENT RESULTS

Table 13: **Full Results on DeepScaleR.** For each metric, the best-performing method is highlighted in **bold**, and the second-best is <u>underlined</u>. Time is the sum of training and generation time of the checkpoint that achieves the best average performance (excluding validation / checkpointing) in hours.

DeepScaleR	Method	MATH500	Olymp.	Minerva Avg@4	AMC23 Avg@32	AIME24 Avg@32	AIME25 Avg@32	Avg.	Time
	π_{ref}	70.2	34.3	29.8	49.1	15.8	8.8	34.7	/
	GRPO	87.2	57.9	45.3	70.1	25.3	22.7	51.4	43.0
Owen2 OD Daga	Pre-filter	86.4	54.6	44.2	69.8	26.9	22.6	50.7	67.4
Qwen3-8B-Base	DS	87.2	55.3	45.7	71.5	24.9	24.2	51.5	69.5
	SPEED	82.4	46.4	40.3	66.6	21.1	15.7	45.5	19.3
	PCL	88.4	56.2	46.8	71.2	25.2	23.9	52.0	<u>41.8</u>
	π_{ref}	65.8	34.4	26.9	47.3	10.9	7.1	32.1	/
	GRPO	83.4	51.0	40.1	60.7	16.1	20.7	45.3	45.5
Owen3-4B-Base	Pre-filter	83.4	47.8	40.0	60.2	18.8	16.2	44.4	39.0
Qwell3-4b-base	DS	83.2	51.6	41.2	62.4	18.5	18.0	45.8	40.1
	SPEED	79.4	45.4	38.3	60.3	15.7	14.5	42.3	10.7
	PCL	83.0	50.6	40.9	60.8	19.4	19.4	<u>45.7</u>	32.8
	π_{ref}	57.0	23.9	21.8	29.0	3.8	1.1	22.8	/
	GRPO	72.4	37.7	31.2	44.9	11.2	6.7	34.0	46.2
Qwen3-1.7B-Base	Pre-filter	74.0	36.5	32.6	45.6	11.7	7.8	34.7	44.2
Qwello-1./b-base	DS	73.2	36.9	31.9	42.7	10.8	7.7	33.9	41.7
	SPEED	73.0	34.4	30.2	37.2	9.2	7.1	31.8	22.7
	PCL	74.4	35.6	31.5	46.3	12.5	9.2	34.9	<u>23.3</u>
	π_{ref}	42.8	12.3	13.8	19.7	4.6	0.4	15.6	/
	GRPO	55.2	23.1	22.6	40.0	13.3	0.0	25.7	47.5
Llama3.2-3B-it	Pre-filter	56.8	24.5	23.3	35.5	16.5	0.7	26.2	44.8
Liama3.2-3B-ii	DS	57.2	23.3	24.1	37.1	17.5	1.0	26.7	40.6
	SPEED	51.4	20.2	20.1	32.0	10.6	0.8	22.5	3.86
	PCL	58.8	23.9	24.0	35.2	15.0	2.1	<u>26.5</u>	28.7

H VALUE MODEL SIZE ABLATION

 We ablate the value model used in PCL across three different model sizes, with results on explained variance of the value prediction shown in Figure 18. Similar to Section 5, we use the average reward of 16 generations for each prompt as the ground-truth p(x). Overall, larger value models exhibit faster convergence compared to smaller ones. On the MATH dataset, all three value models eventually converge to similar performance levels. However, on the larger DeepScaleR dataset, we observe a substantial gap after 100 training steps: the smaller value model significantly underperforms relative to its larger counterparts.

We hypothesize that the smaller value model may require more training steps to reach comparable accuracy and that, given sufficient time, all models could eventually converge to a similar point. Nonetheless, this result highlights the benefit of larger value models in the early stages of training, especially on large-scale datasets.

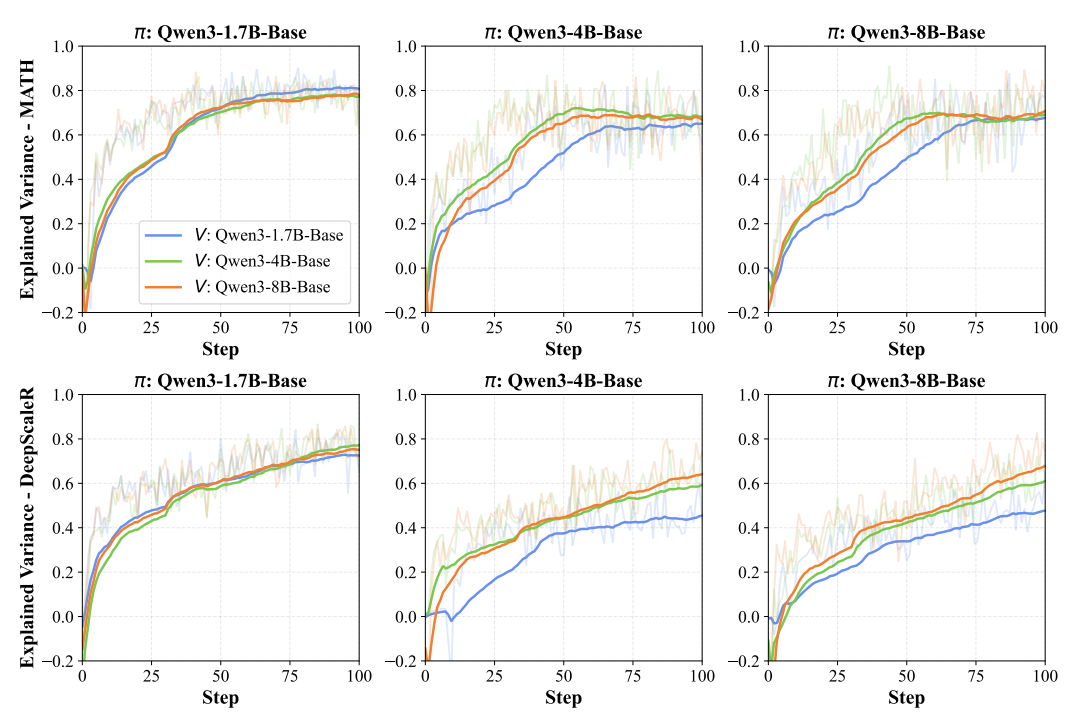


Figure 18: Explained variance on MATH and DeepScaleR with different combinations of Qwen3 base models (1.7B / 4B / 8B) for policy (π) and the value model (V).

I LIMITATIONS

 While PCL demonstrates strong empirical performance across a range of models and datasets, our study has several limitations that open avenues for future work.

Purely on-policy setting. Our experiments are conducted entirely in a purely on-policy RL setting, where new generations are sampled after each policy update. While this simplifies the analysis and avoids additional hyperparameters (e.g., clipping), it may reduce the generalization to more complex training pipelines that leverage off-policy data or replay buffers.

Focus on synchronous setting. Our preliminary investigation and PCL are evaluated in a synchronous training setup where data generation and policy updates are alternated step-by-step. However, many large-scale RL pipelines for LLMs adopt asynchronous architectures for better throughput (Wu et al., 2025; Fu et al., 2025). Extending our analysis and PCL to asynchronous settings may require more sophisticated value model training and prompt selection strategies to handle stale or partially updated policies.

Relatively short context lengths. We limit our experiments to a maximum context length of 4,096 tokens due to compute constraints. While this setting is sufficient for the datasets used (e.g., MATH, DeepScaleR), real-world LLM deployments often involve much longer contexts. From our analysis, for longer context length, the batch size that transitions from sub-linear to linear generation time is larger. Future work could explore the interplay between prompt difficulty, batch decomposition, and context length in long-context regimes.

Limited training horizon. Our experiments are constrained to relatively short training runs (e.g., 2–3 days), which may not fully capture long-term convergence behavior, especially for larger models and datasets. Although we observe strong early-stage performance, it remains an open question whether our analysis in Section 3 would generalize to much longer training runs.